BOREAS An international journal of Quaternary research

Geomorphology, sedimentology and minimum exposure ages of streamlined subglacial landforms in the NW Himalaya, India

SOURAV SAHA, MILAP C. SHARMA, MADHAV K. MURARI, LEWIS A. OWEN AND MARC W. CAFFEE

BOREAS

Saha, S., Sharma, M. C., Murari, M. K., Owen, L. A. & Caffee, M. W.: Geomorphology, sedimentology and minimum exposure ages of streamlined subglacial landforms in the NW Himalaya, India. *Boreas*. 10.1111/bor.12153. ISSN 0300-9483.

Streamlined subglacial landforms that include drumlins in three study areas, the upper Chandra valley around Chandra Tal, the upper Spiti Valley and the middle Yunam Valley of the NW Himalaya of India were mapped and studied using geomorphic, sedimentological and geochronological methods. These streamlined subglacial landforms include a variety of morphological types, including: (i) half egg-shaped forms; (ii) complex superimposed forms; (iii) dome-shaped forms; (iv) inverse forms; and (v) flat-topped symmetrical forms. Sedimentological data indicate that subglacial deformational processes are responsible for the formation of the streamlined subglacial landforms in the Chandra Tal and upper Spiti Valley study areas. In contrast, streamlined landforms in the middle Yunam Valley are the result of melt-out and subglacial erosional processes. In the Yunam Valley study area, 11 new cosmogenic ^{10}Be surface exposure ages were obtained for boulders inset into the crests of streamlined subglacial landforms and moraines, and also for a bedrock surface. The streamlined landforms date to 8–7 ka, providing evidence of an early Holocene valley glaciation, and older moraines date to ~17–15 and 79–52 ka, representing other significant valley glacial advances in the middle Yunam Valley. The subglacial landforms in the Chandra Valley provide evidence for a ≥300-m-thick Lateglacial glacier that advanced southeast, overtopping the Kunzum Range, and advancing into the upper Spiti Valley. The streamlined subglacial landforms in these study areas of the NW Himalaya highlight the usefulness of such landforms in developing glacial chronostratigraphy and for understanding the dynamics of Himalayan glaciation.

Sourav Saha (sahasv@mail.uc.edu) and Lewis A. Owen, Department of Geology, University of Cincinnati, Cincinnati, OH 45221, USA; Milap C. Sharma, Centre for the Study of Regional Development, JNU, New Delhi 110067, India; Madhav K. Murari, Physical Research Laboratory, Navrangpura, Ahmedabad 380009, India; Marc W. Caffee, Department of Physics, Department of Earth, Atmospheric and Planetary Sciences, Purdue University, West Lafayette, IN 47907, USA; *received 11th November 2014, accepted 3rd September 2015.*

The highly dynamic and debris-mantled nature of many Himalayan valley glaciers (Owen & Derbyshire 1989; Benn & Owen 2002) can led to the misconception that these glaciers are unable to produce distinctive subglacial streamlined landforms such as drumlins. However, although not common, drumlins and other streamlined glacial landforms have been described in several regions of the Himalaya (Owen *et al.* 1997, 2001; Pant *et al.* 2005). To address the paucity of information about these landforms, we examined several areas in the Lahul and the Yunam regions of the NW Himalaya of northern India where streamlined glacial landforms are common (Fig. 1). We studied the geomorphic and sedimentary characteristics of the streamlined landforms to help elucidate their mode(s) of formation. We use the term 'streamlined landforms' to refer to drumlins and similar streamlined landforms, reserving the term 'drumlin' for landforms in which the geomorphological and sedimentological evidence unequivocally shows that they are truly drumlins. The objectives of our study were to: (i) describe the general characteristics of the streamlined landforms; (ii) determine their origin, specifically whether or not they were formed by subglacial processes; and (iii) define when the landforms probably formed by developing a local glacial chronostratigraphy using cosmogenic ^{10}Be. In addition, as the orientation of subglacial streamlined landforms generally reflects past ice-flow direction (Trenhaile 1975; Alley *et al.* 1986; Menzies & Rose 1989; Hart 1997; Spagnolo *et al.* 2011; Stokes *et al.* 2011, 2013; Jónsson *et al.* 2014; Yu *et al.* 2015), we used them, together with other geological evidence, including roche moutonnées, striations and clast fabrics, to reconstruct past ice-flow histories and ice dynamics.

Study areas

The Lahul and Yunam regions of the NW Himalaya preserve geomorphic and sedimentary records of past glacier oscillations. These regions are amongst the few places in the Himalaya where preserved glacial landforms indicate piedmont glacier or ice-sheet like behaviour during the past (Owen *et al.* 1997, 2001). Sets of half egg-shaped streamlined hillocks, with individual hillocks tens of metres long and commonly arranged in an *en echelon* pattern, are conspicuous glacial landforms in these regions. We examined the nature of streamlined subglacial landforms in three valleys of the NW Himalaya: (i) the upper Chandra Valley around the Chandra Tal (centred on 32°28.86′N, 77°36.60′E, at altitude ~4300 m a.s.l.); (ii) the upper Spiti Valley (centred on 32°24.66′N, 77°38.58′E, at ~4550 m a.s.l.); and (iii) the middle Yunam Valley (centred on 32°50.46′N, 77°28.68′E, at ~4450 m a.s.l.) (Fig. 1).

DOI 10.1111/bor.12153

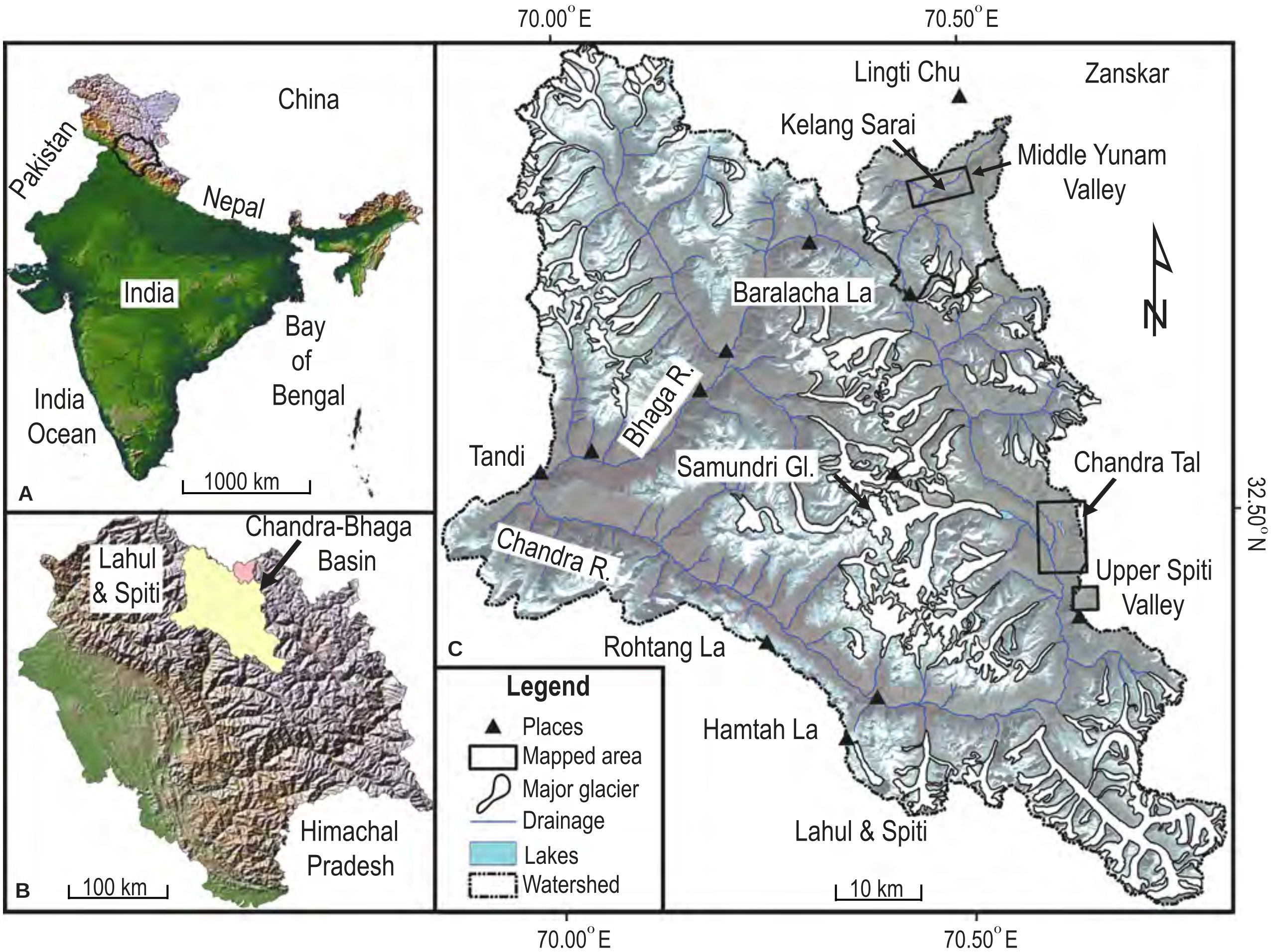

Fig. 1. Location of the study region. A. Map of India including the state of Himachal Pradesh (HP), shown in black. B. Himachal Pradesh showing Chandra-Bhaga and Spiti basins (highlighted in yellow) and Yunam basin (in pink). C. Location map (overlaid on LISS III imagery) showing the major glaciers in the Chandra-Bhaga and Yunam basins of Lahul and Spiti, HP. The three study areas (marked by black rectangles) are the upper Chandra Valley near Chandra Tal, the upper Spiti Valley near Kunzum La and the middle Yunam Valley north of Baralacha La.

The upper Chandra Valley near the Chandra Tal in Lahul is of particular interest because Owen *et al.* (1997, 2001) previously mapped and described the streamlined landforms here as drumlins and stressed their importance for reconstructing the glacial dynamics and the geomorphic history of the region. Pant *et al.* (2005) observed similar landforms in the adjacent Yunam Valley, calling them drumlins on the basis of their morphology. However, comprehensive descriptions of these types of landforms were not provided and descriptions of similar landforms in other regions of the Himalayan-Tibetan orogen are not common.

The Chandra Tal study area in the upper reaches of the Chandra Valley forms a wide intermontane basin with an average width of ~2 km. The valley width remains relatively constant until downstream of Chandra Tal where it becomes steeper, narrows and is more fluvially active. The wider, upper section of the valley is where, during the Lateglacial, the main valley glacier from the Baralacha La (4890 m a.s.l.) joined the westerly tributary Samundri and Dakka glaciers to form a more extensive and thicker glacier (Owen *et al.* 1996, 1997). Both the Chandra Tal and upper Spiti Valley study areas are located north of the northwest-trending Pir Panjal Range and are traversed by the Greater Himalaya. The north-trending Kunzum Range separates the Chandra Tal study area to the west from the upper Spiti study area to the east. Access between these two study areas is through the Kunzum La at 4600 m a.s.l. The Zanskar Range and Greater Himalaya bound the Yunam Valley to the north and south, respectively. The Yunam Valley is ~1 km wide and rises from elevations of >2000 m a.s.l. to peaks that exceed >6000 m a.s.l.

The study areas are located in a transitional climatic zone of the Himalaya between monsoon-influenced southern regions and mid-latitudinal westerlies-influenced northern regions (Owen *et al.* 1995). There is a strong northward aridity gradient across the NW Himalayan region, with the modern snowline increasing northward from ~4800 to ~5500 m a.s.l. (Taylor & Mitchell 2000; Owen & Benn 2005).

Geologically the region is complex, with the South Tibetan Detachment fault (STD) marking an important boundary between Lahul and Spiti to the south and the Yunam Valley to the north. Crystalline rocks of the High Himalayan Crystalline Series outcrop south of the STD. Rocks of the High Himalaya comprise quartzo-feldspathic and phyllitic metasedimentary rocks intruded by Palaeozoic granitoids and Miocene leucogranites. In contrast, Mesozoic sedimentary rocks of the Tethyan Zone are present in the hanging wall and north of the STD. These rocks mostly comprised the Yunam Valley study area, located south of the Zanskar Range (Searle & Fryer 1986; Walker *et al.* 1999; Webb *et al.* 2007).

Chronology of glaciation

Numerical ages for glacial landforms in our three study areas and in adjacent areas of the NW Himalaya are limited (Taylor & Mitchell 2000; Hedrick *et al.* 2011; Owen & Dortch 2014). Of particular relevance to our study is the work of Owen *et al.* (1996, 1997, 2001), who on the basis of geomorphology, morphostratigraphy and cosmogenic ^{10}Be and ^{26}Al exposure dating identified five glacial stages/advances in the Chandra and Bhaga Valleys of Lahul. From oldest to youngest these are: (i) the Chandra glacial stage (not dated); (ii) the Batal glacial stage 15.5 to ~12 ka (Lateglacial); (iii) the Kulti glacial stage 11.4 to ~10.6 ka (early Holocene); (iv) the Sonapani I glacial advance (not dated); and (v) the Sonapani II (~late 19th century) glacial advance. In particular, Owen *et al.* (2001) dated boulders inset into drumlin surfaces to ~11.2 to ~14.0 ka in the Chandra Tal area and assigned them to the Batal glacial stage.

Dortch *et al.* (2013) compiled 685 ^{10}Be ages for the semi-arid western regions of the Himalayan-Tibetan orogen, including glacial stages/advances in the Chandra and Bhaga Valleys. They proposed 19 regional glacial stages since ~300 ka, which they called the semi-arid western Himalayan-Tibetan stages (SWHTS; Table 1). In this study we aimed to date glacial landforms to provide a new glacial chronostratigraphy for the Yunam Valley and to help refine the existing chronostratigraphical framework proposed by Dortch *et al.* (2013) for the western Himalayan-Tibetan regions (Table 1).

Methods

Mapping and geomorphic analysis

High-resolution satellite images (e.g. Google Earth imagery, Google 2009; IRS LISS III, 29th October 2006) and digital elevation models (DEMs) generated from IRS Cartosat-1 stereo pairs (2.5 m) were used to prepare reconnaissance maps for the Chandra Tal and upper Spiti Valley study areas. Beginning with these reconnaissance maps, we constructed geomorphic maps at a scale of 1:10 000 using a handheld GPS (uncertainty ±3 m) to position important landforms. The streamlined and other glacial landforms were mapped and verified in the field by recording multiple waypoints along their crests and margins, and their orientations were recorded by using a compass. These data allowed us to check our remote sensing maps with field data. Our mapping techniques proved to be simple and robust, and they also allowed us to check the field maps produced by Owen *et al.* (1997).

In the valley around Chandra Tal, the a- and b-axes, and the ridge heights of the streamlined landforms were measured using a measuring tape. Determining the b-axes of many of the streamlined landforms here was difficult due to the inaccessibility of the landforms along cliffs. Hence, we only report drumlin elongation ratios (a:b-axis; Trenhaile 1975; Menzies 1979; Benn & Evans 1998; Hättestrand *et al.* 2004; Kerr & Eyles 2007; Clark *et al.* 2009) for the middle Yunam Valley that was relatively accessible. No volumetric analysis of streamlined landforms (cf. Spagnolo *et al.* 2010, 2011; Yu *et al.* 2015) was undertaken in this study.

Sedimentological analysis in the field

The sedimentology of selected streamlined landforms was examined in natural and hand-excavated exposures. Streamlined landforms are few at the northern end of the Chandra Tal study area and where present they are intensely denuded. We did not study the sedimentology of these degraded landforms. In contrast, streamlined landforms are relatively large, well preserved and sporadically distributed towards the southern end of Chandra Tal. We therefore selected landforms for detailed study near Chandra Tal where they were relatively abundant, *en echelon* and strongly aligned, and well preserved. To collect representative sediment samples we chose the most typical half egg-shaped streamlined landforms. As larger streamlined landforms were very hard to hand-excavate to their entire depth we chose five small- to medium-sized landforms to excavate and undertake sedimentological analysis and measure clast fabrics (Table 2). We constructed graphic sedimentary logs, recorded lithofacies descriptions, described particle-size distributions, and measured clast fabrics and clast shapes using the methods of Owen & Derbyshire (1989), Derbyshire & Owen (1997), Benn & Owen (2002) and Knight (1997). The wide areal distribution of sampled landforms in the valley provides us with confidence that our sediment samples are representative of the sedimentology of the streamlined landforms.

Table 1. Glacial chronologies for Ladakh and Zanskar shown with the regional glacial stages (semi-arid western Himalayan-Tibetan stages – SWHTS) of Dortch *et al.* (2013) and synchronous regional glacial stages (monsoonal Himalayan-Tibetan stages – MOHITS) of Murari *et al.* (2014). For details see Owen & Dortch (2014).

Regional glacial stage					
Dortch *et al.* (2013)	Murari *et al.* (2014)	Local glacial stage	Local stage age (ka)	Regional stage age (ka)	Climate correlation
SWHTS 9	MOHITS9	KM-0 stage of Hedrick *et al.* (2011)	311±8	311±32	MIS 9/10
SWHTS 7 (tentative)	MOHITS7	–		234±44 (tentative)	MIS-7/8
SWHTS 6	MOHITS6A	Deshkit 3 stage of Dortch *et al.* (2009)	156±16	146±18	MIS-6, Monsoon and Westerly
SWHTS 5E	MOHITS5E	PM-0 stage of Hedrick *et al.* (2011)	126±8	121±11	MIS-5e, Monsoon
SWHTS 5A	–	Deshkit 2 stage of Dortch *et al.* (2009) Pangong-2 stage of Dortch *et al.* (2013) Ladakh-4 stage of Dortch *et al.* (2013)	86±4 85±15 81±20	80±5	MIS-5a; Monsoon
SWHTS 5A-	–	KM 1–3 stage of Hedrick *et al.* (2011)	72±31	72±8	MIS 4/5a; Monsoon/recession
SWHTS 4	MOHITS4	–	–	61±5	MIS-4; Westerly; Heinrich event-6
SWHTS 3	MOHITS3B	Deshkit 1 stage of Dortch *et al.* (2009) PM-1 stage of Hedrick *et al.* (2011) Pangong-1 stage of Dortch *et al.* (2013)	48±4 47±12 40±3	46±4	MIS-3; Monsoon; Heinrich event-5
SWHTS 2F	MOHITS2G	–	–	30±3	MIS-2; Monsoon; Heinrich event-3
SWHTS 2E	–	Ladakh-2 stage of Dortch *et al.* (2013)	22±3	20±2	MIS-2; Westerlies; gLGM
SWHTS 2D	MOHITS2C	–	–	16.9±0.7	MIS-2; Westerly; Oldest Dryas; Heinrich event-1
SWHTS 2C	MOHITS2B	–	–	14.9±0.8	MIS-2; Westerly; Late Oldest Dryas
SWHTS 2B	–	–	–	13.9±0.5	MIS-2; Westerly; Older Dryas
SWHTS 2A	–	–	–	12.2±0.8	MIS-2; Westerly; Younger Dryas
SWHTS 1E	MOHITS1H	–	N/A	N/A	MIS-1; Monsoon peak1; Climatic Optimum (tentative)
SWHTS 1D	–	–	N/A	N/A	MIS-1; Climatic Optimum (tentative)
SWHTS 1C	MOHITS1E	KM-4 stage of Hedrick *et al.* (2011)	3.9±1.6	3.8±0.6	MIS-1; Westerly
Correlation inconclusive	MOHITS1D	PM-2 stage of Hedrick *et al.* (2011)	2.7±2.3	N/A	MIS-1; Monsoon; Neoglacial
SWHTS 1B	MOHITS1C	Ladakh Cirque of Dortch *et al.* (2013)	1.8±0.4	1.7±0.2	MIS-1; Monsoon; Roman Humid period
SWHTS 1A	MOHITS1C	Pangong Cirque of Dortch *et al.* (2013) PM-3 stage of Hedrick *et al.* (2011)	0.4±0.3 0.3±0.2	0.4±0.1	MIS-1; Westerly; Little Ice Age

In the upper Spiti Valley area, a section was hand-dug through a half egg-shaped streamlined landform (KUN/07/50) and clast fabric analysis was undertaken on this landform. Sand grains from this landform were also sampled for surface texture analysis using scanning electron microscope (SEM). In the middle Yunam Valley, detailed sedimentological and clast fabric analysis were undertaken on two well-exposed road cuts of streamlined landforms, designated as Exposure 1 and Exposure 2 (Table 2).

Clast fabric analysis

Clast fabrics were measured in all the study areas to help determine past ice-flow directions and formation mechanisms (Stanford & Mickelson 1985; Bennett *et al.* 1999; Evans *et al.* 1999; Table 2). We did not observe any thin carapaces of till on the surfaces of the streamlined landforms (Stokes *et al.* 2011) that would indicate postdepositional modification of the sediment. Nevertheless, we removed the upper ≥15 cm of sediment to avoid measuring any sediment that might have experienced postdepositional modification (Hubbard & Glasser 2005; Schomacker *et al.* 2006). This kind of unaltered depositional landform was well suited for fabric measurements and was extensively used in our study. We measured the trend and dip of a-axes of clasts ranging in length from 4 to 14 cm with an a:b-axis ratio of ≥3:2 over an area of 0.25 m^2 (cf. Knight 1997). In the Chandra Tal area, multiple clast fabrics were recorded in the crest of the KG1/DPF streamlined landform at depths of 15 and 60 cm (DPF1; Table 2) and in the side of the streamlined landform IDPF1 at a depth of 15 cm. We also measured the orientation of the lodged boulders in the surfaces of streamlined landforms DPF3 and KUN/07/50 in the Chandra Tal and upper Spiti areas, respectively. Five other clast fabrics were measured at a depth of 15 cm from the crests of the streamlined landforms KG2/DPF, DPF2, KUN/07/50, Exposure 1, and Exposure 2 (Table 2).

Particle size and shape analysis

Sediment samples were collected for particle size and shape analysis, and sand grain surface texture analysis

Table 2. Samples analysed to elucidate the sedimentology of drumlins/streamlined subglacial landforms.

Study site	Sample code	Latitude (°N)	Longitude (°E)	Altitude (m a.s.l.)	Grain size (≤200 μm)	Clast roundness (4–14 cm diameter clasts)	Clast sphericity (4–14 cm diameter clasts)	SEM study of quartz grains	Sample size for SEM study	Fabric analysis	Depth of fabric analysis (cm)	No. of clasts measured for fabric
Chandra Tal area	KG1/DPF[1,2]	32°28.62′	77°36.84′	4303	√	√	√	√	13	√	Below 15	51
	DPF1[1,2]									√	At 60	25
	KG2/DPF[2]	32°27.78′	77°37.02′	4262	√	x	x	√	13	√	Below 15	50
	DPF2[2]	32°28.08′	77°37.02′	4317	√	√	x	√	13	√	Below 15	50
	DPF3[2]	32°28.12′	77°36.78′	4308	x	x	x	x	–	√	Below 15	121
	IDPF1[3]	32°28.62′	77°36.90′	4300	√	√	x	x	–	√	Below 15	50
Upper Spiti area	KUN/07/50[2]	32°24.54′	77°38.28′	4415	√	x	x	√	13	√	Below 15 and surface	25 and 50
Middle Yunam area	Exposure 1[2]	32°50.76′	77°30′	4463	√	x	x	x	–	√	Below 15	50
	Exposure 2[2]	32°50.64′	77°30′	4463	x	x	x	x	–	√	Below 15	41

[1]KG1/DPF and DPF1 are from the same drumlin's surface, but DPF1 was recorded at 45 cm depth from KG1/DPF.
[2]Samples collected from the surfaces of drumlins.
[3]Sample collected from the lee side of drumlin IDPF.
√= samples were used; x = samples were not used/collected.

(Table 2). Clasts larger than granule size were removed in the field. The sediment samples were air-dried in the laboratory for 2–3 days; a few cohesive samples were then carefully disaggregated by hand. Approximately 180 g of each sample was weighed and sieved for 20 min using a motorized shaker in the Geomorphological Laboratory at Jawaharlal Nehru University in Delhi. Particle size data were plotted using GRADISTAT v8 (Blott & Pye 2001). The statistical methods of Folk & Ward (1957) were used to characterize the particle size distributions. The shapes of clasts with a-axes between 4 and 26 cm long were determined in the field, including several clasts examined during the fabric measurements, by measuring their a-, b- and c-axes using a Vernier calliper. Roundness and sphericity were estimated using Power's visual charts (Tucker 1988).

Sand surface textures

Sand surface textures were analysed using SEM from sediment samples collected from the Chandra Tal and upper Spiti Valley study areas (Table 2). Quartz sand grains with diameters of 200–500 μm were identified under an optical microscope and mounted on metal stabs using carbon double sticky tape. The grains were coated with a 20–30 nm thick layer of gold using a sputter conductive gold coating device. An energy dispersive X-ray (EDX) analyser mounted on a scanning electron microscope at the Advance Instrumentation Research Facility at Jawaharlal Nehru University was used to confirm that the sand grains were composed solely of quartz. The surface textures were examined and selective grains were photographed using the secondary electron mode on the SEM and described using the nomenclature of Krinsley & Doornkamp (1973). Thirteen quartz sand grains were examined in each of the four samples (Table 2).

^{10}Be surface exposure dating

Eleven new cosmogenic ^{10}Be ages were determined in this study. Three samples (ZK73–75) were collected from a laterofrontal moraine that encloses an unnamed active glacier ~3 km from the Baralacha La at the headwaters of the Yunam Valley (Fig. 2, Table 3). Five samples were collected from moraines located at the lower stretch of the Yunam Valley, near the confluence with Sarchu River, (ZK61, 64–66, and 69) and two samples (ZK71 and 72) were taken from the streamlined landforms in the middle Yunam Valley (Table 3). Rock glaciers have advanced over some of the moraines in the lower part of the Yunam Valley and care was taken not to collect samples from areas that were affected by rock glaciers. In addition, a rock sample (ZK76) was collected from the glacially polished and striated bedrock at ~200 m above the valley floor.

Large boulders (>1 m in height) were chosen to reduce the possibility that the samples were shielded by snow or were recently exhumed. Samples were collected by chiselling off ~500 g of rock to a depth of ≤5 cm from the tops of the boulder surfaces. Topographical shielding was measured using a handheld inclinometer. Sample preparation was undertaken in the geochronology laboratories at the University of Cincinnati following the methods of Kohl & Nishiizumi (1992), and described in detail in Dortch *et al.* (2009, 2013). This included crushing and sieving the samples to obtain a 250–500 μm particle size fraction. Pure quartz was obtained by treating the sample two to three times with 5% HF/HNO_3 after 10 h of leaching in aqua regia. Other minerals were removed by using lithium heteropolytungstate heavy liquid separation and a Franz magnetic separator. Pure quartz was dissolved in 49% concentrated HF acid after adding low background Be carrier (^{10}Be/^{9}Be of ~1×10^{-15}). Beryllium hydroxide was obtained after fuming with $HClO_4$ acid and passing through anion and cation exchange columns. Two blanks were prepared to assess the Be carrier and laboratory background level of ^{10}Be for each set of samples. The $Be(OH)_2$ was heated in an oven at 750 °C to form BeO, mixed with Nb powder and then loaded into a steel target. The ratios of ^{10}Be/^{9}Be were measured using accelerator mass spectrometry at the Purdue Rare Isotope Measurement Laboratory at Purdue University (Table 3). Currently, there is no agreement on which scaling model is appropriate for the Himalayan-Tibetan region. We therefore present ages using the different scaling models and geomagnetic corrections in Table 3, but use the time-independent model of Lal (1991) and Stone (2000) as advocated in Owen & Dortch (2014) to discuss our new ages.

Results

Geomorphological characteristics

Chandra Tal study area. – Streamlined landforms are abundant in the Chandra Tal study area (Figs 3–5). Of particular note is an area located within the valley west of Chandra Tal (~4280 m a.s.l.) that has small (~20 m) to medium (100s m) sized streamlined landforms on a low ridge (~4300 m a.s.l.). The long-axes of these streamlined landforms are parallel and generally trend between 120 and 150°, with a mean trend of ~135° (Fig. 3C). Long-axis lengths for these streamlined landforms range from 15 to 240 m, with an average length of 58±44 m (1σ uncertainty here and below). The range of heights is small, with an average height of 4±3 m and a maximum of 13 m. Depressions between many of these landforms are partially filled with glacifluvial and colluviated sediments so that their topographical waveform pattern (cf. Spagnolo *et al.* 2012) is not clear and true heights are possibly much

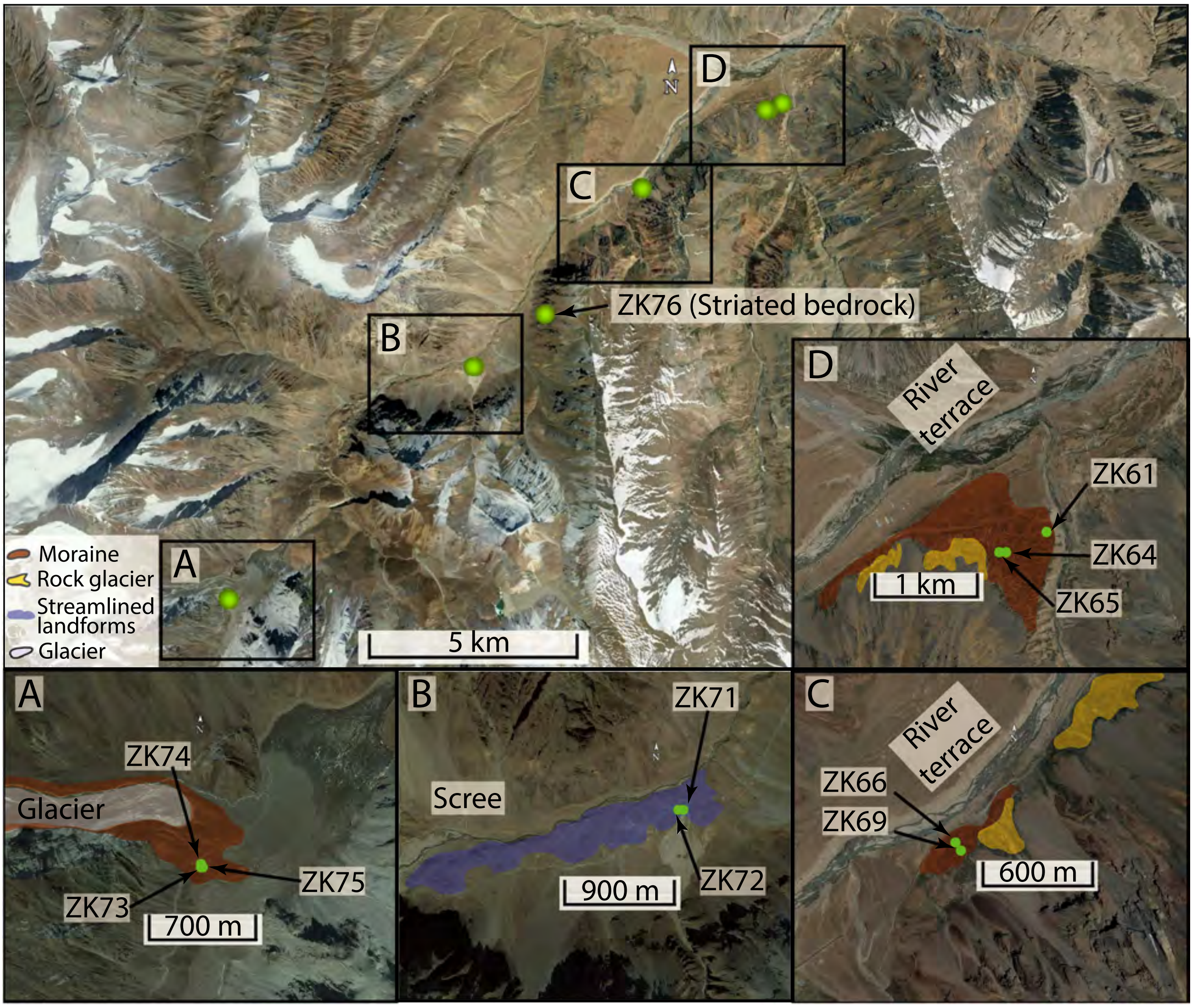

Fig. 2. The Yunam Valley showing detailed study areas for ^{10}Be dating and simplified geomorphology. The red rectangle shows the location of the geomorphic mapping in Fig. 7.

greater. The ridge on which the streamlined landforms are preserved has an average till thickness of ~30 m and is underlain mostly by phyllite and quartzo-feldspathic crystalline rocks. Well-indurated quartzo-feldspathic rocks in this region generally form roche moutonnées (Fig. 3B), whereas extensively cleaved and shattered phyllite bedrock forms subdued mounds.

The streamlined landforms have several distinct morphologies in the Chandra Tal area, which include: (i) half egg-shaped forms, with steeper stoss faces and gentler lee sides (Fig. 5A, Bi); (ii) superimposed forms where one or more streamlined landforms are on top of an older streamlined landform (Fig. 5Bii); (iii) dome-shaped forms that are oval in plan view (Fig. 5Biii); (iv) inverse forms that have reverse geometry with respect to general ice-flow direction, i.e. having a gentler stoss side and steeper lee side (Fig. 5Biv); and (v) flat-topped symmetrical forms that lack distinct stoss and lee faces (Fig. 5Bv). Asymmetrical half egg-shaped (56% of the total 107 streamlined landforms examined; Fig. 5A, Bi) and superimposed landforms (23%), however, are the most common landforms in this area (Fig. 5B top).

Upper Spiti Valley. – The upper Spiti Valley has an average width of ~1.5 km where streamlined landforms are well preserved. Nine half egg-shaped streamlined landforms were mapped in the upper Spiti Valley near Kunzum La (Figs 4, 6A, D, E). Where present, the streamlined landforms are *en echelon* (Fig. 6A), with their long-axes trending 100–110° and are approximately parallel to the SE-trending streamlined landforms in the Chandra Tal study area (Figs 3B, 4). The half egg-shaped streamlined landforms have numerous lodged boulders in their surfaces with the characteristic of gentle stoss and steep lee faces. The lodged boulders are aligned parallel to the long-axes of the stream-

Table 3. Sample numbers, descriptions, locations, ^{10}Be data and ages for glacial landforms in the Yunam Valley (and adjacent) study area.

Sample number	Location	Landform type and context	Boulder size height/width/length (cm)	Lithology	Sample thickness (cm)	Latitude (°N)	Longitude (°E)	Altitude (m a.s.l.)[1]	Topographical correction	^{10}Be concentration (atoms g^{-1} SiO$_2$ × 10^6)[2]	Age time independent Lal (1991)/Stone (2000) (ka)[3]	Age Desilets & Zreda (2003) (ka)[3]	Age Dunai (2000) (ka)[3]	Age Lifton *et al.* (2005) (ka)[3]	Age time dependent Lal (1991)/Stone (2000) (ka)[3]
ZK61	Satu, Yunam Valley	Lateral moraines (KII moraine of Taylor & Mitchell 2000)	150/120/80	Conglomerate	5	32.9058	77.5794	4362	1.090	6.035±0.154	79.0±9.7	76.5±9.4	74.3±7.7	100.1±2.6	87.9±7.9
ZK64	Satu, Yunam Valley	Lateral moraines (KII moraine of Taylor & Mitchell 2000)	200/70/170	Conglomerate	5	32.9041	77.5753	4381	1.090	4.086±0.0653	52.3±6.3	50.5±6.1	48.8±4.9	66.6±1.1	58.6±5.1
ZK65	Satu, Yunam Valley	Lateral moraines (KII moraine of Taylor & Mitchell 2000)	475/200/100	Conglomerate	5	32.9041	77.5746	4382	1.000	4.558±0.109	59.3±7.2	57.7±7.0	55.5±5.7	74.4±1.8	65.4±5.8
ZK66	Tsurap Chu, Yunam Valley	Lateral moraine (Kulti moraine of Taylor & Mitchell 2000)	200/150/90	Sandstone	5	32.8862	77.5402	4438	1.000	0.975±0.026	14.8±1.8	15.1±1.8	14.3±1.5	15.5±0.4	15.2±1.4
ZK69	Tsurap Chu, Yunam Valley	Lateral moraine (Kulti moraine of Taylor & Mitchell 2000)	100/70/100	Quartzite	5	32.8858	77.5405	4422	1.000	1.107±0.045	16.7±2.1	17.0±2.1	16.1±1.7	17.8±0.7	17.3±1.6
ZK71	Tsurap Chu, Yunam Valley	Drumlin, middle Yunam valley	175/100/100	Quartzite	5	32.8449	77.4945	4484	1.000	0.506±0.021	7.9±1.0	8.4±1.0	7.8±0.8	7.8±0.3	7.7±0.7
ZK72	Tsurap Chu, Yunam Valley	Drumlin, middle Yunam valley	250/125/200	Quartzite	5	32.8448	77.4941	4477	1.000	0.435±0.017	6.9±0.9	7.3±0.9	6.8±0.7	6.7±0.3	6.7±0.6
ZK73	Upper Yunam Valley, nr. Baralacha La	Laterofrontal moraine (Sonapani moraine of Taylor & Mitchell 2000)	175/75/50	Quartzite	5	32.7927	77.4293	4757	1.090	0.031±0.005	0.5±0.1	0.5±0.1	0.5±0.1	0.4±0.1	0.5±0.1
ZK74	Upper Yunam Valley, nr. Baralacha La	Laterofrontal moraine (Sonapani moraine of Taylor & Mitchell 2000)	150/60/80	Psammite	5	32.7929	77.4292	4764	1.090	0.044±0.007	0.7±0.1	0.7±0.1	0.7±0.1	0.6±0.1	0.7±0.1
ZK75	Upper Yunam Valley, nr. Baralacha La	Laterofrontal moraine (Sonapani moraine of Taylor & Mitchell 2000)	125/75/40	Psammite	5	32.7929	77.4292	4749	1.090	1.597±0.070	19.8±2.5	19.9±2.5	19.0±2.1	22.1±1.0	21.2±2.0
ZK76	Tsurap Chu, Yunam Valley	Striated bedrock high up valley side	Bedrock	Gneiss	5	32.8568	77.5139	4672	1.000	0.076±0.007	1.2±0.2	1.2±0.2	1.2±0.2	1.1±0.1	1.2±0.1

[1]Altitudes were determined using a handheld GPS with an uncertainty of ±30 m.
[2]Blanks for samples ZK61, 64, 73, 75, 76 = $2.00\pm0.60\times10^{-14}$ and for samples ZK65, 66, 69, 71, 72, 74 = $1.64\pm0.47\times10^{-14}$.
[3]Ages were determined using a rock density of 2.75 g cm^{-3} and 07 KNSTD standard. Uncertainties include analytical and production rate/scale model uncertainties.

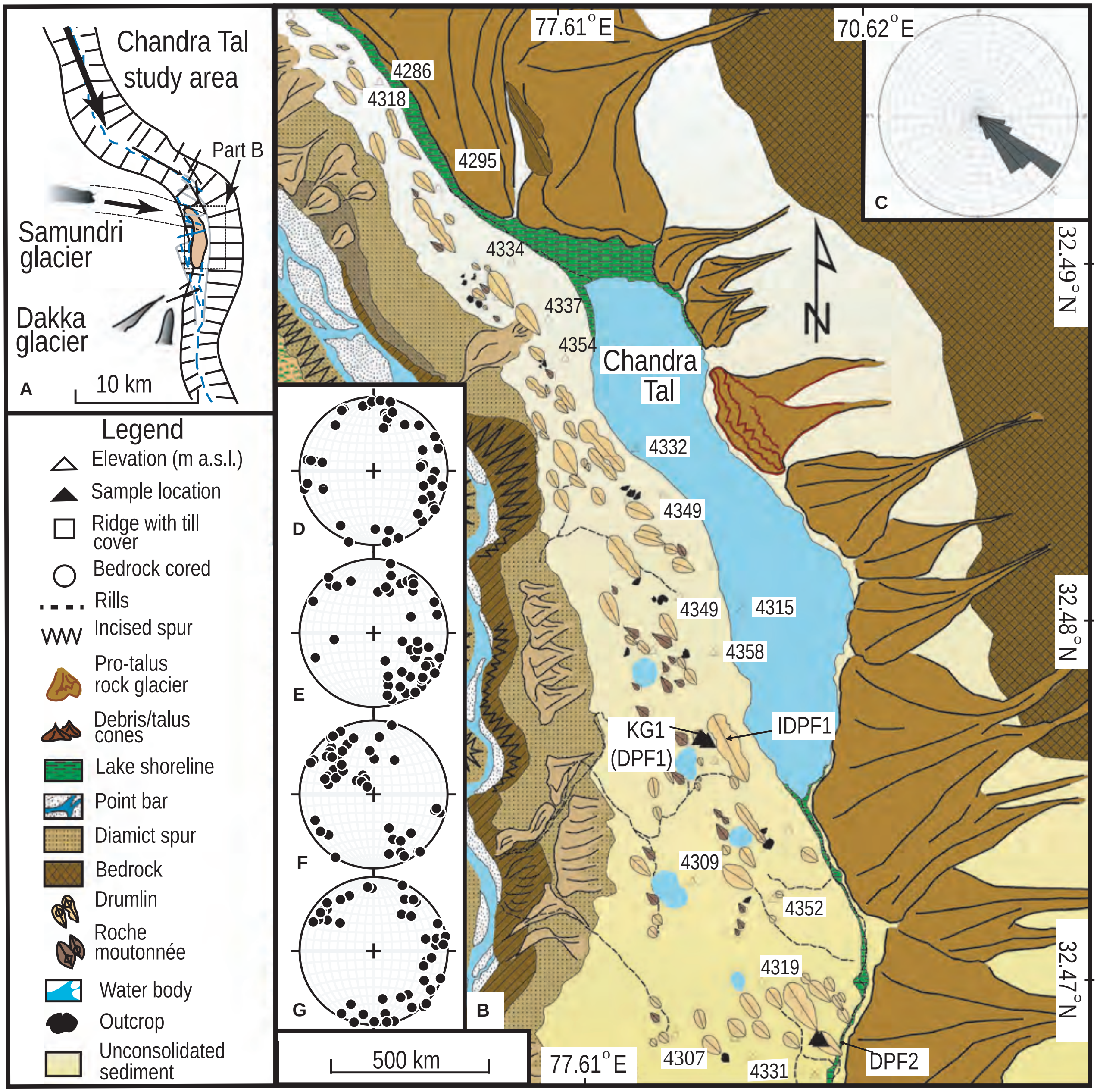

Fig. 3. Geomorphology of the Chandra Tal area. A. Wide intermontane basin with an average width of ~2 km where in the past the main valley glacier from the Baralacha La joined the westerly tributary Samundri glacier. The location of (B) is shown by the dotted rectangle. B. Distribution of streamlined landforms on the low ridge section (~4300 m a.s.l.) west of the Chandra Tal. Complex drumlin symbols (Fig. 5) are used to differentiate classical drumlins from superimposed and other types. C. Rose diagram demonstrating the long-axis trends of mapped drumlins with strong trends between 120 and 150° and a mean of ~135°. D. Parallel and transverse clast fabric patterns of the sample KG1/DPF drumlin. E. Similar parallel fabric of sample IDPF1, measured from the side of a glacier. The deformed diamict matrix has shallow dipping of clasts in both the NW and SE directions, resulting in opposite fabric orientations. F. Similar NW and SE fabric of sample DPF2. G. NW, E and SE fabric of sample KG2/DPF. The clast fabric results support the ice-flow direction inferred from the geomorphic map (B).

lined landforms (Fig. 6A, E). Other streamlined landforms, striations, and glacially polished and ice-moulded bedrock surfaces were mapped and described by Owen *et al.* (1997, 2001) near and on the Kunzum La. These landforms trend in a similar direction (SE) to the streamlined landforms in the upper Spiti Valley (Figs 4, 6).

Middle Yunam Valley. – The Middle Yunam Valley has numerous well-developed streamlined hillocks along the valley floor and is located up to ~12 km downvalley from the present glaciers (Figs 7A, 8A). Moraines and conical hummocky mounds are also present in the valley (Fig. 8B). The long-axes of most streamlined landforms trend NE and are parallel to the valley, but there

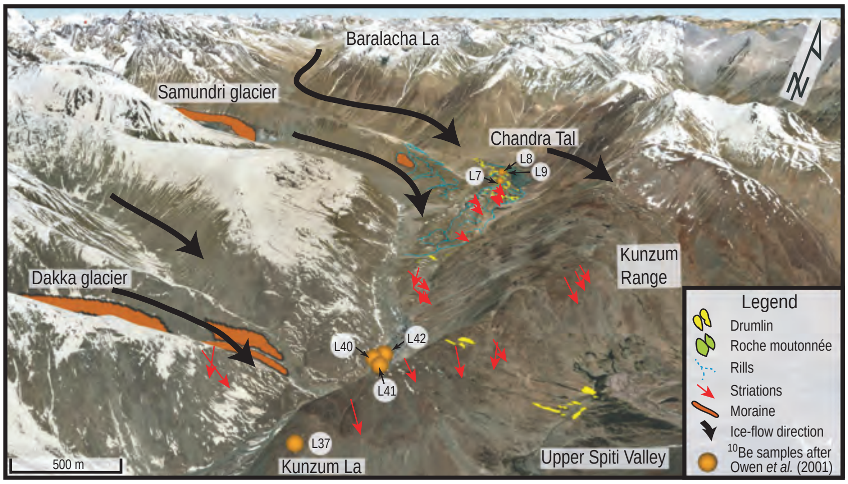

Fig. 4. Google Earth image showing the distribution of striations and drumlins near the Chandra Tal and near or at the Kunzum La (this study and modified after Owen *et al.* 1997). These subglacial features have the same directions as those mapped in Fig. 3. The ^{10}Be sampling sites of Owen *et al.* (2001) are shown. The ages of these samples are as follows; L7: 11.2±0.5 ka; L8: 14.0±0.4 ka; L9: 13.7±0.3 ka; L37: 14.3±0.3 ka; L40: 13.1±0.3 ka; L41: 14.0±0.4 ka; L42: 14.0±0.7 ka.

is a second set of streamlined landforms trending NNE farther down valley (Fig. 7A). The NNE-trending set of streamlined landforms is located close to postglacial debrisflow fans and is aligned along the flow paths of the debrisflow fans. The streamlined landforms have long-axes that range in length from 15 to 240 m with an average of ~68.3±63 m (n = 201). The average height of these landforms is ~15 m and many of these have loose debris on their surfaces. Glacifluvial sands and gravels commonly fill the inter-landform depressions (Fig. 8B). The modal elongation ratio (a:b-axis) for these streamlined landforms is 1:8 (±0.3).

Sedimentological characteristics

Chandra Tal area. – At least 42% (n = 107) of the streamlined landforms examined have diamict cover with ice-polished bedrock cores (Fig. 9). We could not ascertain whether the remaining 58% of the streamlined landforms also have bedrock cores or are composed solely of diamict because they were not excavated. Most of the clasts within the diamicts are striated and are locally derived, composed dominantly of quartzite and phyllite.

The streamlined landforms that were examined are dominantly composed of gravelly sands with a sand and silt to gravel ratio of ~3:2. Laboratory analysis of the sediment samples collected from four different streamlined landforms showed that they are dominantly composed of sand (81–99%) and minor amounts of silt and clay (1–13% coarse silt and <2% of medium-fine silt and clay). Most of these sediment samples that we examined are medium sand-rich and lack finer sediments (Table S1).

Bladed- and elongate-shaped clasts dominate in the analysed sediment samples (Tables S2, S3). Angular and very angular striated (56 and 43%) and subangular (37 and 30%) are most common with minor amounts of subrounded clasts (6 and 13%) in DPF2 and IDPF1 (Table S3). Sub-prismoidal clasts are the dominant sphericity in the diamicts (32%; Table S2).

The clast fabrics are mostly weak to moderately strong, and consist of medium S_1 and very low S_3 eigenvalues ($S_1 \geq 0.5$; Tables 4, S4), i.e. low isotropy and medium to high elongation. The elongated clasts of the KG1/DPF have a slight preferred orientation towards the N and NW, roughly parallel to the long-axes of the streamlined landforms (120–150°; Fig. 3D). Relatively strong NW and SE fabrics are apparent in IDPF1 (Fig. 3E) and DPF2 (Fig. 3F), parallel to their landforms' orientation with a minor transverse component. The clast fabric for KG2/DPF (Fig. 3G) is weak, slightly orientated towards the NW and E. The majority of clasts in analysed samples has very shallow dips (0–20°).

A large variety of sand surface textures is evident (Figs S1, S2, Table S5). In all the samples most of the sand grains have fresh (94%) and conchoidal (97%) fractures (Figs S1, S2, Table S5). Sharp edges (87% of the grains), sharp angular fractures (49%) and low relief surfaces (64%) are also common. Adhering particles (72%), abraded edges and corners (54%), chipped edges, upturned plates (51%), old fractures (41%) and over-printed signatures (41%) are also abundant (Fig. S1, Table S5). Other sand surface textures are present, but they constitute <25% of the total sample.

A drag fold-like pattern is apparent in the lower section of exposure DPF1 (Fig. 10A, B) and several granule size clasts are arranged in a circular pattern around larger clasts, creating a galaxy-like/unidirectional plasmatic fabric pattern within the drag fold (Fig. 10C). This macro-scale galaxy/unidirectional plasmatic-type

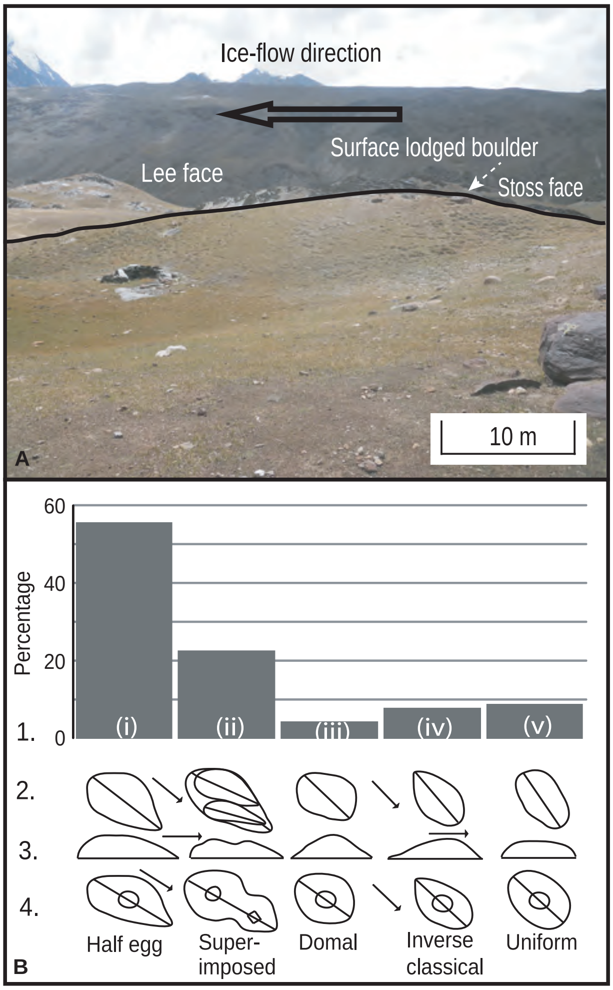

Fig. 5. Characteristics of streamlined landforms. A. Half egg-shaped drumlin (DPF3), with steep up-ice face and gentle down-ice face at Chandra Tal. Large boulders are lodged on its surface, long-axes of which are aligned parallel to the drumlin's long-axis and ice-flow direction (solid arrow). B. Drumlins at Chandra Tal. 1 = frequency of different drumlin types; 2 = zenithal view of outline geometry of morphological types; 3 = azimuthal view of different forms; 4 = map symbols used in Fig. 3B to represent different morphological drumlin forms. Arrows show ice-flow direction.

clast arrangement was carefully measured and is apparent in the fabric at the depth of 60 cm (Fig. 10D). The clasts above the drag fold are jammed together creating grain-bridges/lineaments, and are fractured at a depth of ~15 cm in DPF1 (Fig. 11). The upper section of the layer (~5–10 cm) above the jammed clasts however, is composed of diamict that includes lodged cobbles and small boulders with smooth lee faces and steep stoss faces (Table 2).

Upper Spiti Valley. – The streamlined landform KUN/07/50 examined in detail in the upper Spiti Valley is composed of cobbly matrix-supported massive diamicts, essentially identical to the diamict observed in the streamlined landforms in the Chandra Tal study area. The diamict comprises dominantly sand (91%) with minor amounts of silt and clay (7% coarse silt and <2% of medium-fine silt and clay; Table S1) and has a few striated clasts. Clast fabric at the depth of 15 cm is weak, but with a slight clustering towards the WNW and E, approximately parallel to the general a-axes of the streamlined landform (100–110°). In contrast, the lodged boulders on the surface of the landform are strongly orientated towards the WNW and E (Fig. 6E).

All quartz sand grains examined under the SEM have abundant conchoidal fractures, and fracture faces (85%), sharp edges (77%) and fresh fractures (54%) (Fig. S2). In addition, most of the grains have adhering particles (85%), and abraded edges and corners and low relief surfaces (69%; Fig. S2). Approximately a third of the grains have curved grooves, sharp angular fractures, medium relief, chipped edges and precipitation features.

Middle Yunam Valley. – Crude layering is apparent in the diamicts in the road cuts through the half egg-shaped streamlined landforms in the Yunam Valley (Fig. S3). The diamicts contain subangular to mostly subrounded pebbles and cobbles (84%, n = 50; Table S4) that lack striations. The surfaces of most of these streamlined landforms also consist of loose and weathered sediments. The diamict matrix in Exposure 1 is dominantly composed of fine and medium sand (94%), with minor amounts of coarse silt and clay (6%; Table S1). Clast fabrics examined in Exposure 1 are aligned towards the N, SE, W, and NW (Fig. 7B) and in Exposure 2 the clast fabrics are orientated towards the N, ENW, E, SE, S, and WSW (Fig. 7C).

Glacial chronostratigraphy of the Yunam Valley

We describe our new ^{10}Be ages from NE to SW (older to younger ages) in the Yunam Valley (Fig. 2). To the NE, near the confluence of the Yunam and Sarchu Rivers, ^{10}Be ages were determined for a single moraine ridge that range from ~79 to 52 ka (ZK61, 79.0±9.7; ZK65, 59.3±7.2 ka; ZK64 52.3±6.3 ka; Fig. 2D, Table 3). These ages suggest that the moraine formed during the early part of the Last Glacial (Table 3). Boulders on moraines ~5 km upvalley to the SW from the Yunam–Sarchu confluence yield ages of 16.7±2.1 ka (ZK69) and 14.8±1.8 ka (ZK66), tentatively suggesting an Oldest Dryas or Lateglacial age for moraine formation (Fig. 2C; Table 3). Taylor & Mitchell (2000) assigned these moraines to the Kulti glacial stage. Approximately 7 km upstream from the Yunam–Sarchu confluence, boulders lodged in streamlined landforms yield ages of 7.9±1.0 ka (ZK71) and 6.9±0.9 ka (ZK72) (Fig. 2B), suggesting that the streamlined landforms originated during the early Holocene or perhaps earlier. Close to these samples,

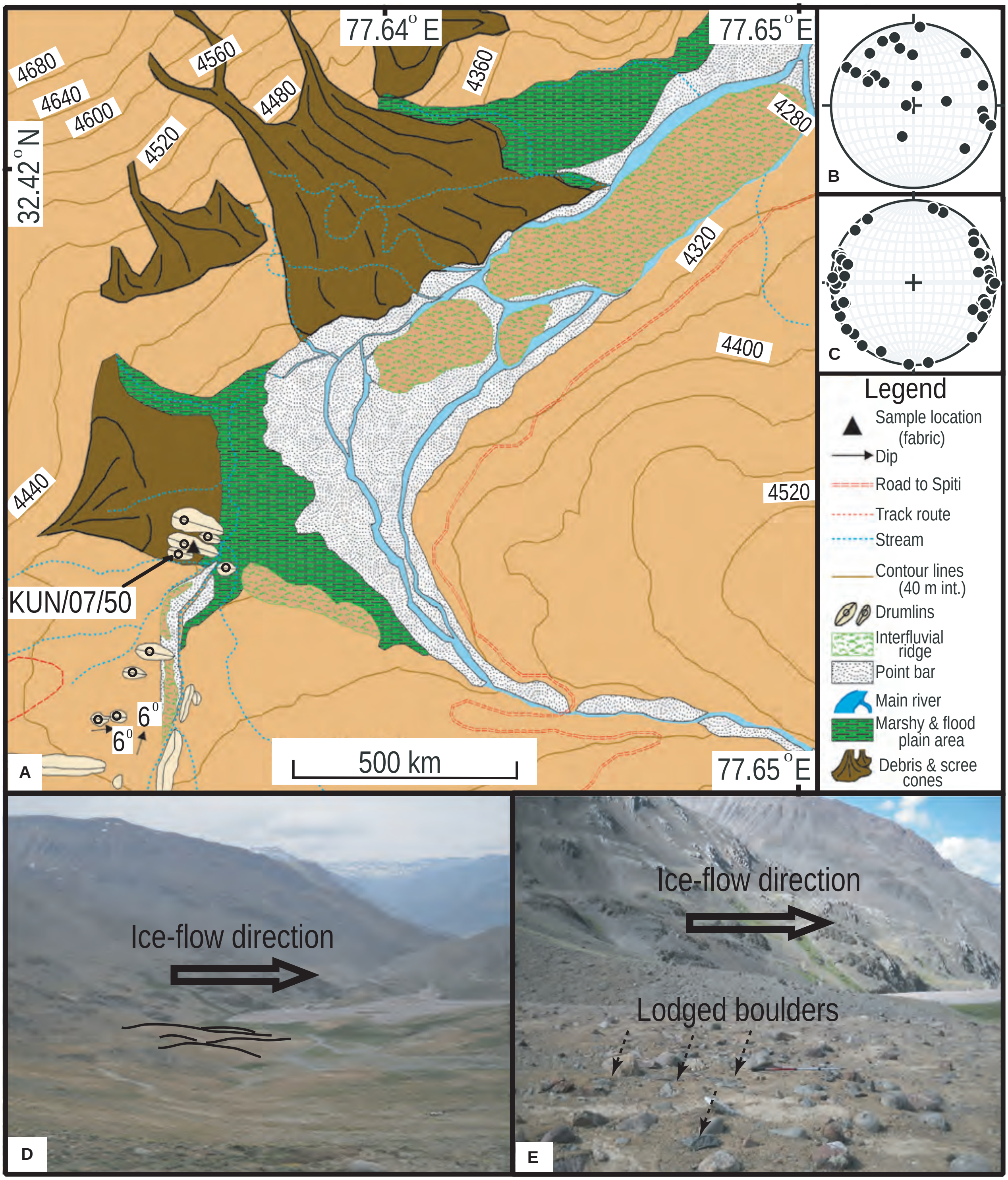

Fig. 6. Geomorphology of the upper Spiti Valley near Kunzum La. A. The spatial distribution and long-axis orientation of streamlined landforms. B. The NW and SE clast fabric pattern of the sample KUN/07/50. This trend is almost parallel to the long-axes of the streamlined landforms shown in (A). C. WNW and ESE trending of lodged boulders on the surface of KUN/07/50. D. Streamlined glacial landforms in the upper Spiti Valley study area. The past ice-flow direction inferred from the dominant orientations of streamlined landforms, clast fabric and striations was toward SE; similar to the main Chandra Valley glacier flow (arrow). E. Gentle stoss-faced and steep lee-faced small boulders lodged extensively at the surface of the streamlined landform KUN/07/50 at the upper Spiti Valley. Long-axes of these boulders are strongly orientated towards the SE.

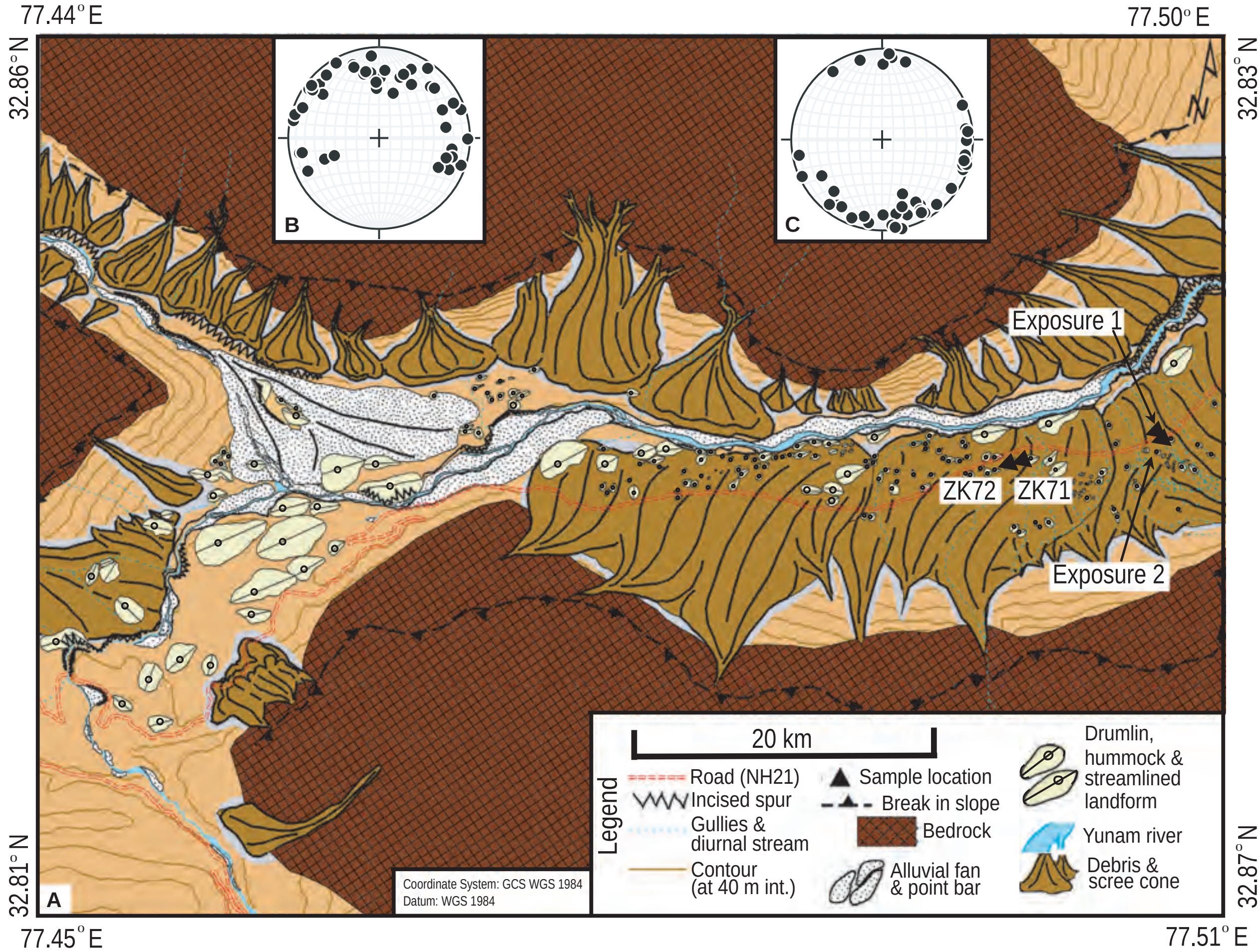

Fig. 7. Geomorphic map of the middle Yunam Valley (location in Fig. 1). A. Distribution of streamlined landforms exhibiting two sets of flow directions, with the dominant flow towards the NE. Another set is oblique to transverse to the dominant orientation. Postdepositional debrisflow processes extensively modify the latter. B. Clast fabric at Exposure 1 showing alignment towards the N, SE, W and NW. C. Clast fabrics for Exposure 2 trend towards the N, ENE, E, SE, S and WSW. Clast fabrics are very weakly developed in the diamict matrix of these landforms.

sample ZK76 from striated bedrock high up the valley side, yields a ^{10}Be age of 1.2±0.2 ka (Fig. 2). We argue that this age is anomalously young given its morphostratigraphical position, and its fresh nature suggests that it may have recently been exhumed from beneath a layer of till. Ages for boulders on a laterofrontal moraine, close to Baralacha La to the SW, range between ~20 and 0.5 ka (19.8±2.5 ka, ZK75; 0.7±0.1 ka, ZK74; and 0.5±0.1 ka, ZK73; Fig. 2A). Taylor & Mitchell (2000) assigned this laterofrontal moraine to the Sonapani glacial advance (without differentiating between the Sonapani I and II stages). The older ^{10}Be exposure age (ZK75) however, is probably a consequence of inherited ^{10}Be from prior exposure. The young ages are consistent with the morphostratigraphical position of the moraine being adjacent to the active ice. We acknowledge that our sampling set is not large, but given the stratigraphical coherence, with moraines getting progressively younger upvalley towards the contemporary glaciers, we argue that the ages provide a good representation of the timing of glaciation.

Discussion

Interpretation of streamlined landforms

Chandra Tal study area. – In the Chandra Tal study area the majority of the streamlined landforms (56%; n = 107) is classic half egg-shaped drumlin forms, although a variety of other streamlined geometric forms were also identified and mapped. The existence of a wide range of streamlined morphological types in a single drumlin field has been reported from other areas and appears to be more common a phenomenon than previously acknowledged (Wright 1957; Finch & Walsh 1973; Knight 1997; Knight & McCabe 1997; Meehan *et al.* 1997; Zelcs & Dreimanis 1997; Benn & Evans 1998; Kerr & Eyles 2007; Clark *et al.* 2009; Spagnolo *et al.* 2010, 2011, 2012). The long-axes of the

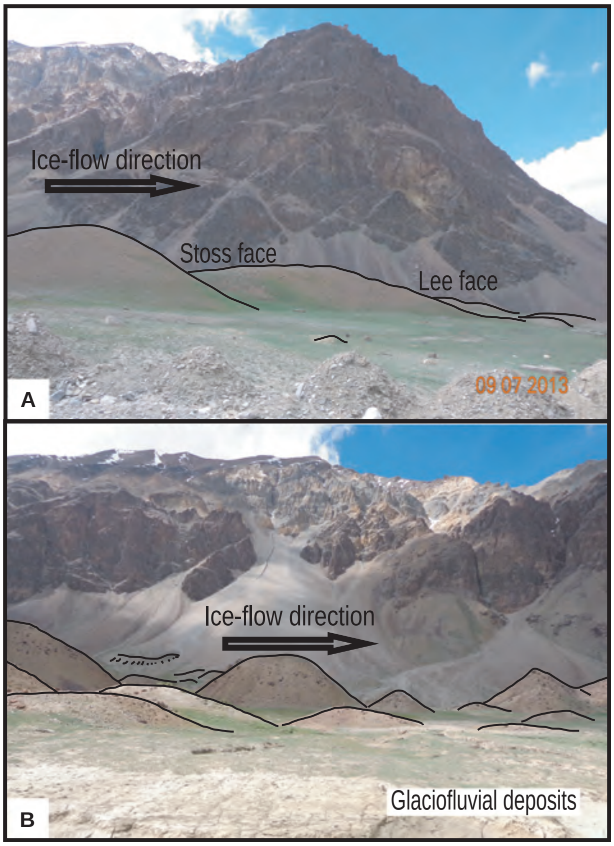

Fig. 8. Streamlined landforms in the middle Yunan Valley. A. Classic drumlin forms with well-developed steep stoss and gentle lee faces. B. Large variations in sizes of streamlined hillocks.

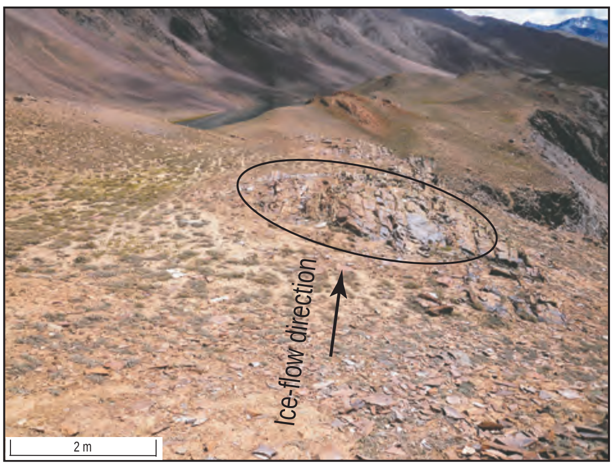

Fig. 9. Ice-polished and striated bedrock observed at the ridge highs of the drumlins in the Chandra Tal study area (in black ellipsoid). These drumlins are cored by these bedrock ridges, which are also aligned in the same directions as the long-axes of the drumlins. The bedrock ridges probably acted as obstacles to the ice flow and favoured drumlin formation.

streamlined landforms in the Chandra Tal study area are predominantly aligned toward ~135° (Fig. 3C) and striations mapped on glacially polished bedrock surfaces in this region and roche moutonnées also trend toward the SE (Figs 3B, 4). The streamlined landforms have large cobbles and boulders inset into their surfaces, mostly on their lee-sides. These large cobbles and boulders have gentle stoss and steep lee faces, and their long-axes also align parallel to long-axes of the streamlined landforms. The streamlined landforms are generally very small in their lengths but their average height is comparable to similar streamlined landforms reported from other areas (Spagnolo *et al.* 2012; Yu *et al.* 2015). The streamlined landforms at Chandra Tal are composed of poorly sorted, matrix-supported massive diamict with locally derived striated clasts, characteristics commonly observed in glacial deposits. Half of the clasts are angular but subangular clasts make up about a third of the diamict and are also common to glacial settings (Stokes *et al.* 2011). SEM analysis of surface textures of quartz sand grains further provides evidence of glacial abrasion, plucking and grinding by displaying grooving, chipped edges and adhering angular particles (Fig. S1, Table S5; Krinsley & Donahue 1968; Krinsley & Doornkamp 1973; Whalley & Langway 1980; Mahaney 1990; Mahaney *et al.* 1991; Mahaney & Andres 1991; Mahaney *et al.* 1996; Helland & Holmes 1997; Mahaney & Kalm 2000). The galaxy/unidirectional plasmatic fabric-type structures present in the lower part of DPF1 are similar to those that are commonly reported from thin sections of subglacially deformed till (Hart 1995; Menzies *et al.* 1997; Hiemstra & Rijsdijk 2003; Evans *et al.* 2006) and probably are produced during ductile deformation (Fig. 10A). Towards the surface of the same exposure, however, brittle deformation structures are present including clast jamming, grain bridging and fracturing (Fig. 11). The surface layer is composed of firmly lodged boulders and cobbles, which probably formed under englacial and subglacial conditions and suggest subglacial lodgement/deformation processes during the final stage of formation (Hart 1997; Knight 1997; Knight & McCabe 1997; Meehan *et al.* 1997; Hiemstra & Rijsdijk 2003; Evans *et al.* 2006; Stokes *et al.* 2013). The moderate to weak clast fabric (S_1 and S_3 eigenvalues) apparent in all our samples (Table 4) also indicates that subglacial deformation processes produced these streamlined landforms (Dowdeswell & Sharp 1986; Hicock 1991; Hart 1995; Stokes *et al.* 2011). In summary, the sedimentological evidence supports the view that the diamict is a subglacial deformation till and the streamlined landforms near Chandra Tal are true drumlins. Most of these drumlins overlie glacially polished and striated bedrock ridges and are identical to part bedrock/part till type of Stokes *et al.* (2011, 2013). These bedrock knobs probably acted as obstacles to glacier flow and localizing pressure melting of the

Table 4. Clast fabric patterns with respect to the long-axes of streamlined landforms and their vector analysis.

Study site	Sample name	General long-axis orientation of drumlins	Preferred orientation w.r.t. magnetic north	Preferred orientation w.r.t. long-axis of drumlins	Eigen vectors			Eigen values		
					V_1	V_2	V_3	S_1	S_2	S_3
Site 1	KG1/DPF	NW to SE (120–150°)	NW to SE and NNW	Parallel and transverse	353.7	86	227.7	0.49	0.425	0.084
	DPF1	NW to SE (120–150°)	NE to SW and NW	Parallel and transverse	–	–	–	–	–	–
	KG2/DPF	NW to SE (120–150°)	NW to SE and E	Parallel	131.7	40.7	242.1	0.55	0.362	0.088
	DPF2	NW to SE (120–150°)	NW to SE	Parallel	316.3	178.6	53.7	0.628	0.208	0.164
	DPF3	NW to SE (120–150°)	NW to SE	Parallel	–	–	–	–	–	–
	IDPF1	NW to SE (120–150°)	NW to SE	Parallel	135.4	36.1	254	0.573	0.315	0.112
Site 2	KUN/07/50	NW to SE (100–110°)	NW to SE	Parallel	313.7	72.1	201.9	0.597	0.261	0.143
Site 3	Exposure 1	SW to NE and NNE	Diffuse	Diffuse	283.1	14.3	188	0.51	0.413	0.078
	Exposure 2	(100–110°)	Diffuse	Diffuse	169.6	2.24	336.1	0.59	0.368	0.042

glacier ice (Hart 1997; Knight 1997; Zelcs & Dreimanis 1997). Using the nomenclature of Clark (2010) the Chandra Tal bedrock-cored drumlins may be described as obstruction drumlins.

Upper Spiti Valley. – The streamlined landforms in the upper Spiti Valley have similar geomorphic characteristics to the obstruction drumlins in the Chandra Tal study area and they have similar orientations. The streamlined landforms mapped at and near the Kunzum Range trend between 100 and 110° (Fig. 6) and striations mapped on the Kunzum Range also trend to the SE (Fig. 4), approximately parallel to the SE-trending drumlins in the Chandra Tal study area. The lodged boulders on the surfaces of the streamlined landform in the upper Spiti Valley similarly align toward the SE (Fig. 6E).

The characteristics of the sediment composing streamlined landform KUN/07/50 are similar to those of the sediment in the drumlins in the Chandra Tal study area. SEM analysis of sand grains also provides evidence of glacial abrasion, grinding and plucking (Fig. S1, Table S5). Weak clast fabrics indicate similar deformation of the sediment in the upper Spiti Valley as observed in the adjacent Chandra Tal area. The presence of lodged boulders and cobbles inset into the surface of the streamlined landforms also supports the view that the lodgement/deformational processes produced this diamict (Evans *et al.* 2006). We interpret the diamict in the upper Spiti Valley as subglacial till and the streamlined landforms here as drumlins.

Middle Yunam Valley. – Most streamlined landforms in the middle Yunam Valley trend towards the NNE,

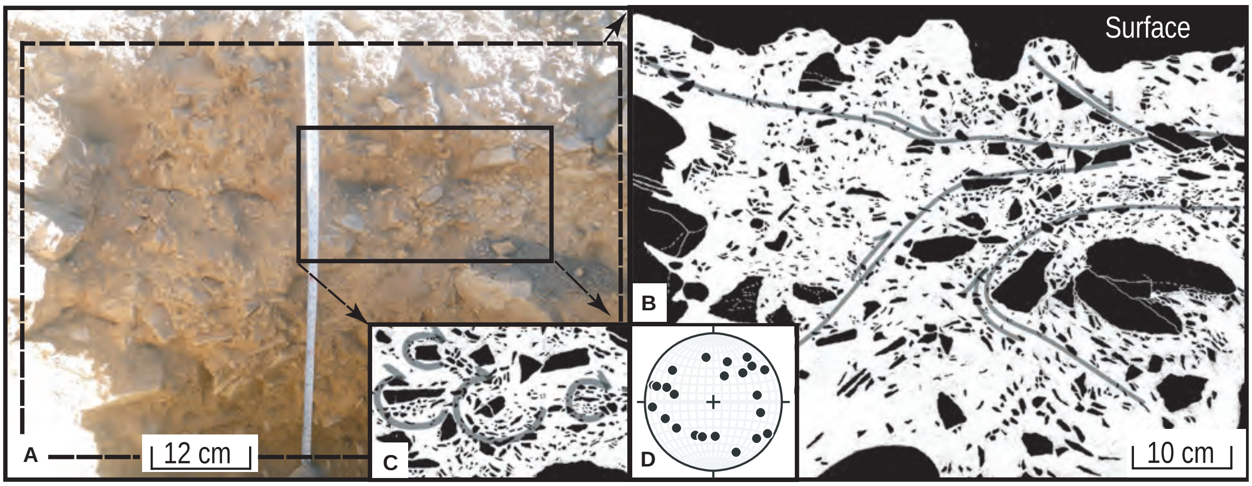

Fig. 10. Sedimentology of DPF1 (the same sample location was used for clast fabric measurements at 60 cm depth and named as KG1/DPF). A. View of an excavation in the lee of the landform. B. Drag fold-like pattern of clast distribution at the bottom, and clast jamming and grain fracturing towards the top in an otherwise massive structure. C. Galaxy/unidirectional plasmatic fabric-type rotation of smaller grains (granules) around larger ones (pebbles) evident in the exposure and shown with inferred direction of rotation. D. Lower hemisphere stereonet at the lower-middle section of the exposure also indicates multiple clast orientations supporting the galaxy/unidirectional plasmatic fabric-type rotation in the diamict matrix.

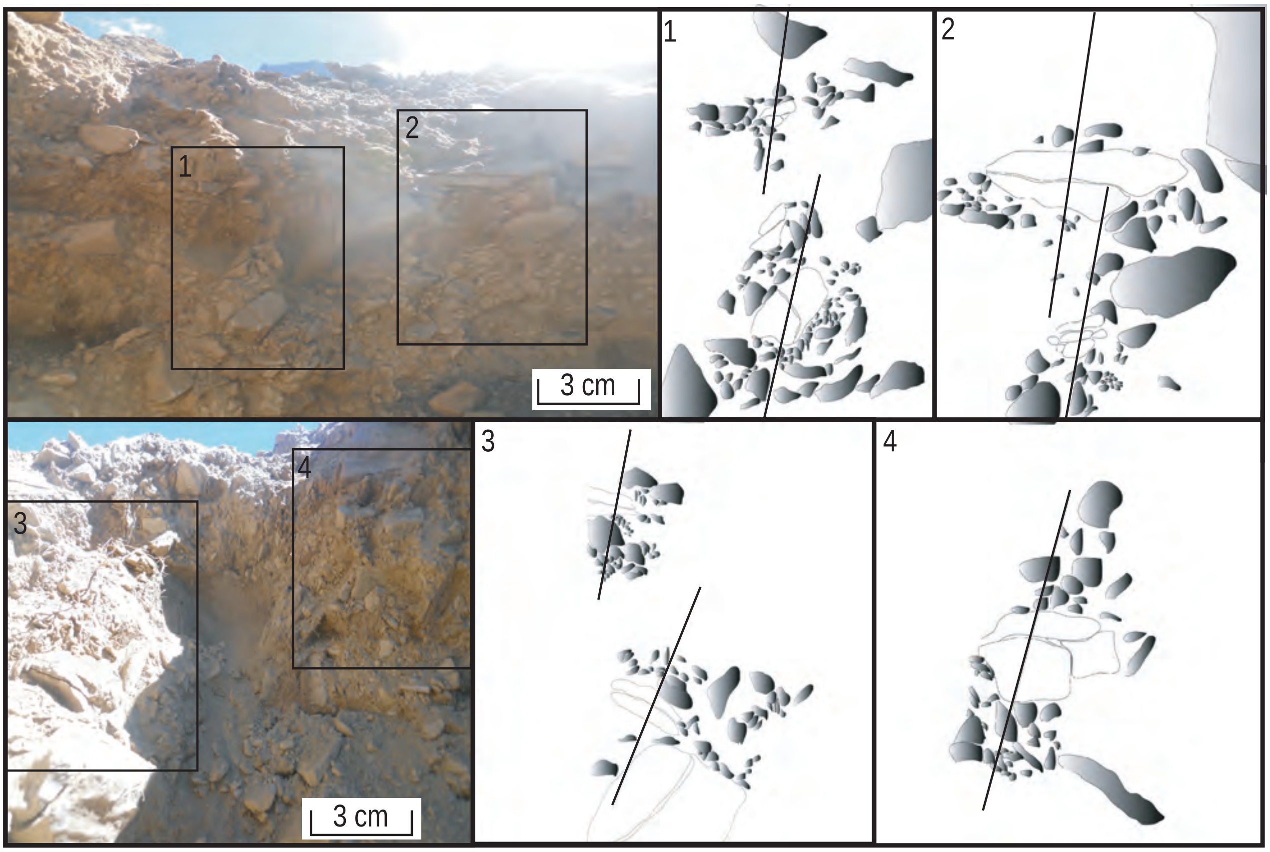

Fig. 11. Typical brittle deformation of clasts ~15 cm below the surface at KG1/DPF. Grain bridging/lineament is well developed and fracturing of clasts occurs along the plane of weakness of the grains.

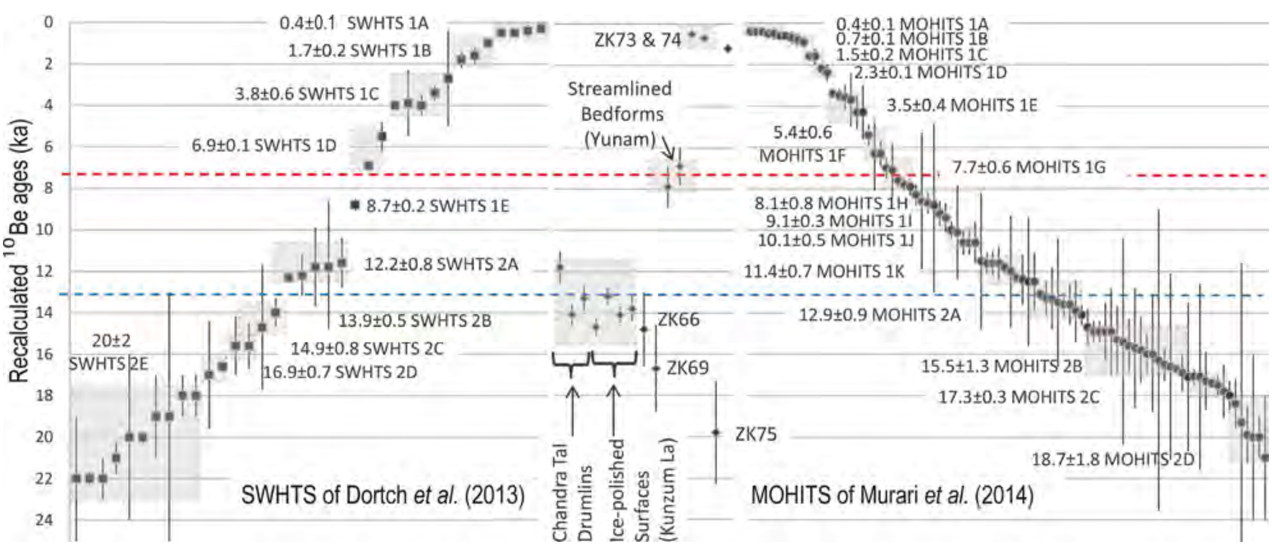

Fig. 12. Age plots for glacial stages in the Himalayan-Tibetan orogen from 24 ka to present (Owen & Dortch 2014) and possible comparison of timing of glaciations with the regional glacial stages adapted from Dortch *et al.* (2013) and Murari *et al.* (2014). These ^{10}Be ages were recalculated using CRONUS-Earth online calculators-Version 2.2. ^{10}Be age clusters are labelled by grey (dotted box) rectangles and Semi-arid Western Himalayan-Tibetan Stages (SWHTS) of Dortch *et al.* (2013) to the left and Monsoonal Himalayan-Tibetan Stages (MOHITS) of Murari *et al.* (2014) to the right are also shown on the y-axis. The ^{10}Be ages of the streamlined landforms (Yunam) of this study and the ^{10}Be ages of drumlins at Chandra Tal area and ice-polished surfaces of Kunzum La of Owen *et al.* (2001) are also shown (middle column) for comparison. The dotted line shows the minimum ages of drumlins/streamlined subglacial landforms in Chandra Tal (blue) and middle Yunam (red) study areas.

parallel to the valley length (Fig. 7). The streamlined landforms in the middle Yunam Valley include classic half egg-shaped streamlined forms, hummocks and lateral moraines. The classic half egg-shaped streamlined landforms in this area have comparable elongation ratios and geomorphology to drumlins reported elsewhere in the world (Trenhaile 1975; Menzies 1979; Benn & Evans 1998; Hättestrand *et al.* 2004; Kerr & Eyles 2007; Clark *et al.* 2009), but they are distinct from the obstruction drumlins in the Chandra Tal and upper Spiti Valleys. These streamlined forms have loose debris on their surfaces and are interfingered with hummocky mounds. As they all have similar debris cover on their surfaces and glacifluvial deposits in their depressions, they probably formed at the same time. These characteristics may also indicate ice-marginal influence at their final stage of formation during deglaciation in the valley. Morphologically they are not as distinctive as the drumlins in the adjacent valleys so they may be transitional between true drumlins and ice-marginal landforms. The crude layering in the diamict, developed by a concentration of clasts parallel to the present valley floor, is similar to structures common in melt-out tills (Fig. S3; Evans *et al.* 2006). Most of the clasts are subrounded with no striations. The fabric, however, is only weakly developed in the matrix, in contrast to the characteristics of classic melt-out till (Evans *et al.* 2006). These clast fabrics were measured from streamlined landforms that were located in the lower reaches of the study area parallel to the debris-flow fans there. Postdepositional erosional processes probably have modified the clast fabrics (Fig. 7A). No bedrock cores were evident within these streamlined landforms. Based on our sedimentological data, the diamict in the middle Yunam Valley may be interpreted as melt-out till. The crudely developed layers in the melt-out till must have been eroded by the overriding glacier in the stoss and lee faces in its later stage to form the present half egg-shaped morphology. This suggests that the current morphology of drumlins/streamlined landforms is the result of both glacial depositional and erosional processes.

Glacial dynamics and regional ice-flow history

Drumlins mapped and examined in the Chandra Tal and upper Spiti study areas were probably formed within a single glacier system. Based on the orientations of drumlins, lodged cobbles and boulders on drumlin surfaces, clast fabrics within the drumlins, and other palaeoglacial records, including the orientations of roche moutonnées and striations, we conclude that the regional ice-flow direction in the Chandra Tal and upper Spiti study areas was towards the SE.

The widening of the Chandra Valley into an intermontane basin near the Chandra Tal (Fig. 3A) would have allowed glaciers to spread out from the Baralacha La and from the tributary Samundri and Dakka Valleys (Fig. 3A) to create a larger and thicker (≥300 m) glacier near Chandra Tal. The wide opening of the valley and distribution of streamlined landforms, ice-polished bedrock surfaces, and striations both on the valley bottom and on ridges, for example, on the Kunzum Range, suggest that the Chandra glacier may have become more like a piedmont glacier that spread out towards the SE (Figs 3, 4). The SE trend of this glacier may indicate a former valley course distinct from the contemporary S-trending Chandra Valley, and/or a valley glacier that was so thick that it over-spilled its valley (Fig. 4).

In contrast, in the middle Yunam Valley the streamlined landforms indicate valley-parallel flow and a relatively thinner (~40 m based on the height of moraines) glacier. Based on the extent of ice-marginal streamlined landforms in the Yunam Valley, the glacier probably advanced ~12 km from the contemporary glacier terminus.

Chronological constraint and palaeoenvironmental interpretation

Owen & Dortch (2014) discussed the challenges of using exposure ages to define glacial chronologies in the Himalayan-Tibetan orogen. As noted by Owen & Dortch (2014), large spreads of TCN ages determined from sets of boulders collected from single landforms are probably due to geological factors such as erosion, exhumation and boulder instability. Our ages are likewise subject to uncertainties associated with geological factors, as well as uncertainties related to scaling factors.

The ^{10}Be ages obtained for boulders on the moraine ridges near the confluence of the Yunam and Sarchu Rivers indicate that glaciers advanced in this area during the early part of the Last Glacial (~79.0±9.7 to 52.3±6.3 ka), and may be synchronous with Heinrich events 5 and 6; these correspond to the glacial stages SWHTS5A (tentative; MIS 5a), SWHTS5A- (MIS 4/5a), SWHTS4 (MIS 4) and/or SWHTS3 (MIS 3) of Dortch *et al.* (2013) (Fig. 12). This timing suggests that glacial advance in the Yunam Valley was forced by monsoon systems as suggested by Dortch *et al.* (2013). ^{10}Be ages determined for the moraines in the Tsarap Chu Valley south of Yunam of 16.7±2.1 and 14.8±1.8 ka tentatively suggest an advance during the Oldest Dryas and/or termination during the Lateglacial. These ages are close to the SWHTS2D and SWHTS2C regional glacial stages of Dortch *et al.* (2013) and suggest that this younger glaciation was probably influenced by mid-latitudinal westerlies.

Based on ^{10}Be ages obtained from boulders inset in drumlins in the Chandra valley and from polished bedrock at Kunzum La, Owen *et al.* (2001) showed that glaciation was extensive in the Chandra and Bhaga Valleys during the Lateglacial at ~15.5–12 ka (the Batal stage). Dortch *et al.* (2013) proposed three distinct glacial advances during this time (SWHTS2A, 2B and 2C). Murari *et al.* (2014) for the monsoon-influenced regions of the Himalaya and Tibet proposed two glacial advance/stages for this time, which they called Monsoonal Himalayan-Tibetan Stages 2A (MOHITS2A) and 2B (MOHITS2B). However, because of insufficient data we cannot assign our moraines and drumlins to a distinct glacial stage of Dortch *et al.* (2013) and/or Murari *et al.* (2014). The two drumlins that we dated in the middle Yunam Valley yield ^{10}Be ages of 7.9±1.0 and 6.9±0.9 ka and may be synchronous with the SWHTS1E and SWHTS1D of Dortch *et al.* (2013) and/or MOHITS1G and MOHITS1H of Murari *et al.* (2014) (Fig. 12). Based on these exposure ages, it is probably that the main valley glacier advanced before 8–7 ka and that the drumlins and other streamlined landforms may have formed before or during the early Holocene.

Drumlins in areas north and south of Baralacha La ice divide appear to have formed at different times. Their ^{10}Be exposure ages reflect the deglaciation in both the valleys and can give a more comprehensive picture of local glacial chronostratigraphy when used in conjunction with moraine ages.

Conclusions

Geomorphic and sedimentological analyses of streamlined landforms in three study areas in the NW Himalaya of northern India support the view that these landforms are drumlins. While in general the drumlins in the Chandra Tal and upper Spiti Valleys can be described as obstruction drumlins, the transitional complex drumlins in the middle Yunam Valley are probably to have been formed by both depositional and erosional processes. The streamlined landforms that we studied are highly variable in terms of morphological types and lengths, but are smaller in length than typical drumlins associated with ice sheets. Their average height however, is similar to drumlins in other areas of the world. Sedimentological data suggest that the drumlins in the Chandra Tal and upper Spiti Valleys are formed by subglacial deformation. In contrast, the drumlins in the Yunam Valley consist of melt-out till later shaped by ice flow. The geomorphic evidence suggests that the main Chandra trunk valley glacier was thick (≥300 m) and flowed SE in the upper reaches of the Chandra valley during the Lateglacial and overtopped the Kunzum Range at or near Kunzum La to spread in to the upper Spiti Valley. In contrast, a valley-parallel glacier formed the streamlined landforms in the Yunam Valley.

The new glacial chronostratigraphy in the Yunam Valley defines the timing of four glacial advances: (i) during the early part of the Last Glacial, ~79.0±9.7 to 52.3±6.3 ka; (ii) during the Oldest Dryas and/or during the Lateglacial, 16.7±2.1 and 14.8±1.8 ka; (iii) during the early Holocene, 7.9±1.0 and 6.9±0.9 ka; and (iv) during the Little Ice Age. These glacial advances became progressively more restricted over time and were asynchronous with glacial advances in the adjacent Chandra-Bhaga Valleys. During the early Holocene, sometime before 8–7 ka, the main Yunam Valley glacier possibly advanced ~12 km from its present position.

Our study of the streamlined subglacial landforms of the NW Himalaya highlights the usefulness of such landforms in developing glacial chronostratigraphy. Moreover these landforms provide useful information for understanding the dynamics of Himalayan glaciation.

Acknowledgements. – This work was a part of S. Saha's M.Phil dissertation at the Jawaharlal Nehru University and supported by the University Grant Commission, India. Sincere thanks to the Editor Professor Jan A. Piotrowski, reviewer Dr M. Trommelen and an anonymous reviewer for their constructive and useful comments on an earlier version of the manuscript that helped to greatly improve it. S. Saha expresses sincere thanks to Dr Ruchita Pal for helping with the SEM analysis and Dr V. K. Raina for scrutinizing his M.Phil work. Thanks also to the Centre for the Study of Regional Development for organizing a summer fieldtrip. We also thank Prof. Craig Dietsch for his insightful comments. M. Caffee acknowledges support from NSF EAR-1153689.

References

Alley, R. B., Blankenship, D. D., Bentley, C. R. & Rooney, S. T. 1986: Deformation of till beneath ice stream B, West Antarctica. *Nature 322*, 57–59.

Benn, D. I. & Evans, D. J. A. 1998: *Glaciers and Glaciation*. 820 pp. Edward Arnold, London.

Benn, D. I. & Owen, L. A. 2002: Himalayan glacial sedimentary environments: A framework for reconstructing and dating former glacial extents in high mountain regions. *Quaternary International 97–98*, 3–26.

Bennett, M. R., Waller, R. I., Glasser, N. F., Hambrey, M. J. & Huddart, D. 1999: Glacigenic clast fabrics: genetic fingerprint or wishful thinking? *Journal of Quaternary Science 14*, 125–135.

Blott, S. J. & Pye, K. 2001: Gradistat: a grain size distribution and statistics package for the analysis of unconsolidated sediments. *Earth Surface Processes and Landforms 26*, 1237–1248.

Clark, C. D. 2010: Emergent drumlins and their clones: from till dilatancy to flow instabilities. *Journal of Glaciology 51*, 1011–1025.

Clark, C. D., Hughes, A. L. C., Greenwood, S. L., Spagnolo, M. & Ng, F. S. L. 2009: Size and shape characteristics of drumlins, derived from a large sample, and associated scaling laws. *Quaternary Science Reviews 28*, 677–692.

Derbyshire, E. & Owen, L. A. 1997: Quaternary glacial history of the Karakoram Mountains and Northwest Himalayas: a review. *Quaternary International 38–39*, 85–102.

Desilets, D. & Zreda, M. 2003: Spatial and temporal distribution of secondary cosmic-ray nucleon intensities and applications to in situ cosmogenic dating. *Earth and Planetary Science Letters 206*, 21–42.

Dortch, J. M., Owen, L. A. & Caffee, M. W. 2013: Timing and climatic drivers for glaciation across semi-arid western Himalayan Tibetan orogen. *Quaternary Science Reviews 78*, 188–208.

Dortch, J. M., Owen, L. A., Haneberg, W. C., Caffee, M. W., Dietsch, C. & Kamp, U. 2009: Nature and timing of large-landslides in northern India. *Quaternary Science Reviews 28*, 1037–1056.

Dowdeswell, J. A. & Sharp, M. J. 1986: Characterization of pebble fabrics in modern terrestrial glacigenic sediments. *Sedimentology 33*, 699–710.

Dunai, T. J. 2000: Scaling factors for production rates of *in situ* produced cosmogenic nuclides: a critical reevaluation. *Earth and Planetary Science Letters 176*, 157–169.

Evans, D. J. A., Phillips, E. R., Hiemstra, J. F. & Auton, C. A. 2006: Subglacial till: formation, sedimentary characteristics and classification. *Earth-Science Reviews 78*, 115–176.

Evans, D. J. A., Salt, K. & Allen, C. S. 1999: Glacitectonized lake sediments, Barrier Lake, Kananaskis Country, Canadian Rocky Mountains. *Canadian Journal of Earth Sciences 36*, 395–407.

Finch, T. F. & Walsh, M. 1973: Drumlins of County Clare. *Biological, Geological, and Chemical Science 73*, 405–413.

Folk, R. L. & Ward, W. C. 1957: Brazos River Bar – a study in the significance of grain size parameters. *Journal of Sedimentary Petrology 27*, 3–26.

Hart, J. K. 1995: Drumlin formation in southern Anglesey and Arvon, northwest Wales. *Journal of Quaternary Science 10*, 3–14.

Hart, J. K. 1997: The relationship between drumlins and other forms of subglacial glaciotectonic deformation. *Quaternary Science Reviews 16*, 93–107.

Hättestrand, C., Götz, S., Näslund, J., Fabel, D. & Stroeven, A. P. 2004: Drumlin formation time: evidence from northern and central Sweden. *Geografiska Annaler 86*, 155–167.

Hedrick, K. A., Seong, Y. B., Owen, L. A., Caffee, M. W. & Dietsch, C. 2011: Towards defining the transition in style and timing of Quaternary glaciation between the monsoon-influenced Greater Himalaya and the semi-arid Transhimalaya of Northern India. *Quaternary International 236*, 21–33.

Helland, P. E. & Holmes, M. A. 1997: Surface textural analysis of quartz sand grains from ODP Site 918 off the southeast coast of Greenland suggests glaciation of Southern Greenland at 11 Ma. *Palaeogeography, Palaeoclimatology, Palaeoecology 135*, 109–121.

Hicock, S. R. 1991: On subglacial stone pavements in till. *Journal of Geology 99*, 607–619.

Hiemstra, J. F. & Rijsdijk, K. F. 2003: Observing artificially induced strain: implications for subglacial deformation. *Journal of Quaternary Science 18*, 373–383.

Hubbard, B. & Glasser, N. 2005: *Field Techniques in Glaciology and Glacial Geomorphology.* 400 pp. John Wiley and Sons, England.

Jónsson, S. A., Schomacker, A., Benediktsson, Í. Ö., Ingólfsson, Ó. & Johnson, M. D. 2014: The drumlin field and the geomorphology of the Múlajökull surge-type glacier, central Iceland. *Geomorphology 207*, 213–220.

Kerr, M. & Eyles, N. 2007: Origin of drumlins on the floor of Lake Ontario and in upper New York State. *Sedimentary Geology 193*, 7–20.

Knight, J. 1997: Morphological and morphometric analyses of drumlin bedforms in the Omagh Basin, North Central Ireland. *Geografiska Annaler 79*, 255–266.

Knight, J. & McCabe, A. M. 1997: Drumlin evolution and ice sheet oscillations along the NE Atlantic margin, Donegal Bay, western Ireland. *Sedimentary Geology 111*, 57–72.

Kohl, C. P. & Nishiizumi, K. 1992: Chemical isolation of quartz for measurement of in-situ produced cosmogenic nuclides. *Geochimica et Cosmochimica Acta 56*, 3583–3587.

Krinsley, D. H. & Donahue, J. 1968: Environmental interpretation of sand grain surface textures by electron microscopy. *Geological Society of America Bulletin 79*, 743–748.

Krinsley, D. H. & Doornkamp, J. C. 1973: *Atlas of Quartz Sand Surface Textures.* 91 pp. University Press, Cambridge.

Lal, D. 1991: Cosmic ray labeling of erosion surfaces: *in situ* nuclide production rate sand erosion models. *Earth and Planetary Science Letters 104*, 429–439.

Lifton, N. A., Bieber, J. W., Clem, J. M., Duldig, M. L., Evenson, P., Humble, J. E. & Pyle, R. 2005: Addressing solar modulation and long-term uncertainties in scaling secondary cosmic rays for in situ cosmogenic nuclide applications. *Earth and Planetary Science Letters 239*, 140–161.

Mahaney, W. C. 1990: Glacially-crushed quartz grains in late Quaternary deposits in the Virunga Mountains, Rwanda - indicators of wind transport from the north? *Boreas 19*, 81–89.

Mahaney, W. C. & Andres, W. 1991: Glacially crushed quartz grains in loess as indicators of long-distance transport from major European ice centers during the Pleistocene. *Boreas 20*, 231–239.

Mahaney, W. C. & Kalm, V. 2000: Comparative scanning electron microscopy study of oriented till blocks, glacial grains and Devonian sands in Estonia and Latvia. *Boreas 29*, 35–51.

Mahaney, W. C., Claridge, G. & Campbell, I. 1996: Microtextures on quartz grains in tills from Antarctica. *Palaeogeography, Palaeoclimatology, Palaeoecology 121*, 89–103.

Mahaney, W. C., Vaikmae, R. & Vares, K. 1991: Scanning electron microscopy of quartz grains in supraglacial debris, Adishy Glacier, Caucasus Mountains, USSR. *Boreas 20*, 395–404.

Meehan, R. T., Warren, W. P. & Gallagher, C. J. D. 1997: The sedimentology of a Late Pleistocene drumlin near Kingscourt, Ireland. *Sedimentary Geology 111*, 91–105.

Menzies, J. 1979: A review of literature on the formation and location of drumlins. *Earth Science Reviews 14*, 315–359.

Menzies, J. & Rose, J. 1989: Subglacial bedforms—an introduction. *Sedimentary Geology 62*, 117–122.

Menzies, J., Zaniewski, K. & Dreger, D. 1997: Evidence of microstructures, of deformable bed conditions within drumlins, Chimney Bluffs, New York State. *Sedimentary Geology 111*, 161–175.

Murari, M. K., Owen, L. A., Dortch, J. M., Caffee, M. W., Dietsch, C., Fuchs, M., Haneberd, W. C., Sharma, M. C. & Townsend-Small, A. 2014: Timing and climatic drivers for glaciation across monsoon-influenced regions of the Himalayan-Tibetan orogen. *Quaternary Science Reviews 88*, 159–182.

Owen, L. A. & Benn, D. I. 2005: Equilibrium-line altitudes of the Last Glacial Maximum for the Himalaya and Tibet: an assessment and evaluation of results. *Quaternary International 138*, 55–78.

Owen, L. A. & Derbyshire, E. 1989: The Karakoram glacial depositional system. *Zeitschrift für Geomorphologie N.F., Supplement76*, 33–73.

Owen, L. A. & Dortch, J. M. 2014: Nature and timing of Quaternary glaciation in the Himalayan-Tibetan orogen. *Quaternary Science Reviews 88*, 14–54.

Owen, L. A., Bailey, R. M., Rhodes, E. J., Mitchell, W. A. & Coxon, P. 1997: Style and timing of glaciation in the Lahul Himalaya, northern India: a framework for reconstructing late Quaternary palaeoclimatic change in the western Himalayas. *Journal of Quaternary Science 12*, 83–109.

Owen, L. A., Benn, D. I., Derbyshire, E., Evans, D. J. A., Mitchell, W. A., Thompson, D., Richardson, S., Lloyd, M. & Holden, C. 1995: The geomorphology and landscape evolution of the Lahul Himalaya, Northern India. *Zeitschrift für Geomorphologie N.F. 39*, 145–174.

Owen, L. A., Derbyshire, E., Richardson, S., Benn, D. I., Evans, D. J. A. & Mitchell, W. A. 1996: The Quaternary glacial history of the Lahul Himalaya, northern India. *Journal of Quaternary Science 11*, 25–42.

Owen, L. A., Gualtieri, L., Finkel, R. C., Caffee, M. W., Benn, D. I. & Sharma, M. C. 2001: Cosmogenic radionuclide dating of glacial landforms in the Lahul Himalaya, northern India: defining the timing of Late Quaternary glaciations. *Journal of Quaternary Science 16*, 555–563.

Pant, R. K., Phadtare, N. R., Chamyal, L. S. & Juyal, N. 2005: Quaternary deposits in Ladakh and Karakoram Himalaya: a treasure trove of the palaeoclimate records. *Current Science 88*, 1789–1798.

Schomacker, A., Kruger, J. & Kjær, K. H. 2006: Ice-cored drumlins at the surge-type glacier Bruarjokull, Iceland: a transitional-state landform. *Journal of Quaternary Science 21*, 85–93.

Searle, M. P. & Fryer, B. J. 1986: Garnet and muscovite-bearing leucogranites, gneisses, and migmatites of the Higher Himalaya from Zanskar, Kulu, Lahoul, and Kashmir. *Collision Tectonics 19*, 185–201.

Spagnolo, M., Clark, C. D. & Hughes, A. L. C. 2012: Drumlin relief. *Geomorphology 153–154*, 179–191.

Spagnolo, M., Clark, C. D., Hughes, A. L. C. & Dunlop, P. 2011: The topography of drumlins; assessing their long profile shape. *Earth Surface Processes and Landforms 36*, 790–804.

Spagnolo, M., Clark, C. D., Hughes, A. L. C., Dunlop, P. & Stokes, C. R. 2010: The planar shape of drumlins. *Sedimentary Geology 232*, 119–129.

Stanford, S. D. & Mickelson, D. M. 1985: Till fabric and deformational structures in drumlins near Waukesha, Wisconsin, U.S.A. *Journal of Glaciology 31*, 220–228.

Stokes, C. R., Fowler, A. C., Clark, C. D., Hindmarsh, R. C. A. & Spagnolo, M. 2013: The instability theory of drumlin formation and its explanation of their varied composition and internal structure. *Quaternary Science Reviews 62*, 77–96.

Stokes, C. R., Spagnolo, M. & Clark, C. D. 2011: The composition and internal structure of drumlins: complexity, commonality, and implications for a unifying theory of their formation. *Earth Science Reviews 107*, 398–422.

Stone, J. O. 2000: Air pressure and cosmogenic isotope production. *Journal of Geophysical Research 105*, 23753–23759.

Taylor, P. J. & Mitchell, W. A. 2000: The Quaternary glacial history of the Zanskar Range, north-west Indian Himalaya. *Quaternary International 65–66*, 81–99.

Trenhaile, A. S. 1975: The morphology of a drumlin field. *Annals of the Association of American Geographers 65*, 297–312.

Tucker, M. E. 1988: *Techniques in Sedimentology.* 394 pp. Blackwell Scientific Publications, Oxford.

Walker, J. D., Martin, M. W., Bowring, S. A., Searle, M. P., Waters, D. J. & Hodges, K. V. 1999: Metamorphism, melting, and extension: age constraints from the High Himalayan slab of southeast Zanskar and northwest Lahul. *The Journal of Geology 107*, 473–495.

Webb, A. A. G., Yin, A., Harrison, T. M., Celerier, J. & Burgess, W. P. 2007: The leading edge of the Greater Himalaya Crystalline complex revealed in the NW Indian Himalaya: implications for the evolution of the Himalayan orogen. *Geology 35*, 955–958.

Whalley, W. B. & Langway, C. C. Jr 1980: A scanning electron microscope examination of subglacial quartz grains from Camp Century core, Greenland - A preliminary study. *Journal of Glaciology 25*, 125–131.

Wright, H. E. Jr 1957: Stone orientation in Wadena drumlin field, Minnesota. *Geografiska Annaler 39*, 19–31.

Yu, P., Eyles, N. & Sookhan, S. 2015: Automated drumlin shape and volume estimation using high resolution LiDAR imagery (Curvature Based Relief Separation): a test from the Wadena Drumlin Field, Minnesota. *Geomorphology 246*, 589–601.

Zelcs, V. & Dreimanis, A. 1997: Morphology, internal structure and genesis of the Burtnieks drumlin field, Northern Vidzeme, Latvia. *Sedimentary Geology 111*, 73–90.

Supporting Information

Additional Supporting Information may be found in the online version of this article at http://www.boreas.dk.

Fig. S1. Surface texture analysis of quartz sand grains using scanning electron microscope (SEM).

Fig. S2. Percentages of surface textural types observed using SEM on quartz sand grains (200–500 μm particle size fraction and sample size = 52).

Fig. S3. The road-cut exposure (Exposure 1) located in Fig. 6 showing ablation till composition. The photograph was taken from the extreme right of the stoss face of the postdepositional modified drumlin, which is transverse to the valley. The white plastic scale is 15 cm long.

Table S1. Particle size distribution data.

Table S2. Clast a-axis (principal), b-axis (intermediate) and c-axis (short) length data.

Table S3. Clast roundness and sphericity data, recorded following Power's visual chart.

Table S4. Clast fabric data and statistical results.

Table S5. Different types of surface textures observed using SEM on quartz sand grains (200–500 μm in diameter).